R-1686
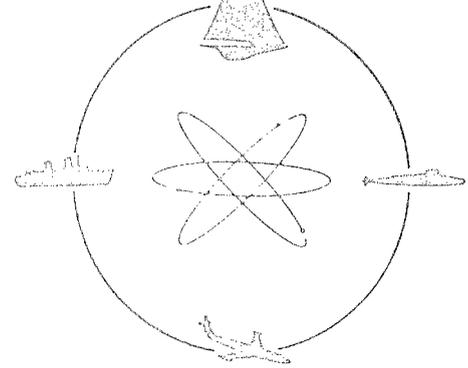
426

DAVIDSON
LABORATORY

Report SIT-DL-74-1686

February 1974

MATHEMATICAL MODEL OF WHEELED VEHICLES
EXITING FROM THE
RIVERINE ENVIRONMENT

by

M. P. Jurkat

STEVENS INSTITUTE
OF TECHNOLOGY

CASTLE POINT STATION

HOBOKEN, NEW JERSEY 07030

DAVIDSON LABORATORY
Stevens Institute of Technology
Castle Point Station
Hoboken, New Jersey 07030

Report SIT-DL-73-1686

February 1974

MATHEMATICAL MODEL OF WHEELED VEHICLES
EXITING FROM THE
RIVERINE ENVIRONMENT

by

M. P. Jurkat

Prepared for

U. S. Army Tank-Automotive Center
under
Contract DAAE07-73-C-0056
(DL Project 4026/453)

Approved for public release;
distribution unlimited.

Approved:

I. Robert Ehrlich, Manager
Transportation Research Group

60 pages
20 figures

R-1686

ABSTRACT

A two-dimensional, vertical-plane, computer simulation model describing the dynamics of a wheeled vehicle exiting from the riverine environment is presented. The model includes the effects of soft soil, suspensions, buoyancy, drive train characteristics and the inertial reactions of the unsprung masses. The body is modeled as a composite of rectangular sections; the tires are rigid. The stream bottom and bank surface can be any specified arbitrary geometry; their soil properties are specified by the land locomotion soil value system.

KEYWORDS

River Crossings
Mobility
Amphibians
Off-Road Vehicles
Computer Simulation

ii

TABLE OF CONTENTS

LIST OF FIGURES

I. INTRODUCTION

The philosophy and initial efforts in simulating the exiting of an off-road vehicle from a body of water was presented by Sloss, Ehrlich and Worden[1] in the second volume of a series of reports[2,3] on general studies of vehicles in the riverine environment. These reports defined the total river-crossing problem as being composed of ingress, water performance and egress. The egress portion, being the most difficult, was considered in need of the most urgent analytic study.

In response to this need, a simple, vertical plane computer simulation model was written and validated with a small vehicle in the idealized environment of a laboratory river simulator. This model was restricted to rigid, planar banks, consisting of only a single ramp. The surface-wheel interaction was modeled by a single spring-damper wheel deflection mechanism, the tire-surface coefficient of friction and the bank slope.[1]

Muddappa and Baker[4] attempted to extend this model by including more general soil-wheel interactions based on the land locomotion soil value system. However, since this model employed only equilibrium equations, it could not truly simulate dynamic situations.

The model described herein is, basically, an extension of the Sloss-Ehrlich-Worden model. It extends the simulation to arbitrarily shaped banks with arbitrary soil parameters, but it restricts the wheel to being solid. The inclusion of flexible wheels awaits the development of flexible wheel models which are capable of simulating travel over both hard, rough terrain and soft soils.

Since it is anticipated that this simulation will be used to describe motion over both obstacles and hard terrain, a much more complete set of motion equations, including many inertial terms ignored in the earlier models, are included.

A major feature required for simulation of wheel-soil interaction is the calculation of wheel slip. This required the complete dynamic modeling of the forces tending to spin the wheels, including those from the engine-drive train, soil shear resistance, and hydrodynamic drag on the spinning submerged tire. Thus the model presented here represents a major increase in sophistication over previous efforts.

II. MODEL DESCRIPTION

The Vehicle

The vehicle is treated as a multi-mass system consisting of a body and any number of axles.[*] The entire vehicle is treated symmetrically in the lateral direction and is therefore assumed restricted in roll, sway and yaw. This results in a vertical plane simulation allowing only three degrees of freedom: surge (x), heave (z) and pitch (θ). Figure 1 presents the coordinate system employed, using a two-axle vehicle as an example.

The axles are assumed to be thin rods with their associated unsprung mass concentrated on a line connecting the left and right wheels. The wheels, attached to the axles at each end, are assumed to have rectangular cross-sections and are allowed only to translate in the vehicle heave (z) direction. All wheels are constrained to rotate together so that only one wheel rotational degree of freedom is allowed; thus the vehicle is assumed to have all-wheel drive with no differential between front and rear axles. Due to the left-right assumption of symmetry, both wheels of an axle rotate at the same speed.

The vehicle body is considered to consist of a number[**] of rectangular boxes with rectangular cross section. These boxes and the wheel assemblies generate buoyant forces when submerged. For linear motion the entire mass of the body is assumed to be concentrated at its center of gravity.

The axles are joined to the body by a spring, damper and bump-stop system (see Figure 2). Multiple rates for the spring and both bump stops are allowed. The damper is assumed to have different rates and blow-off forces for jounce and rebound, but to be only velocity dependent.

---

[*]Currently, for convenience, the simulation is restricted to 8 axles or a 16x16 vehicle; however, this restriction is easily removed without compromising the integrity of the model.

[**]Currently, up to ten.

FIGURE 1. SIMULATION SCHEMATIC
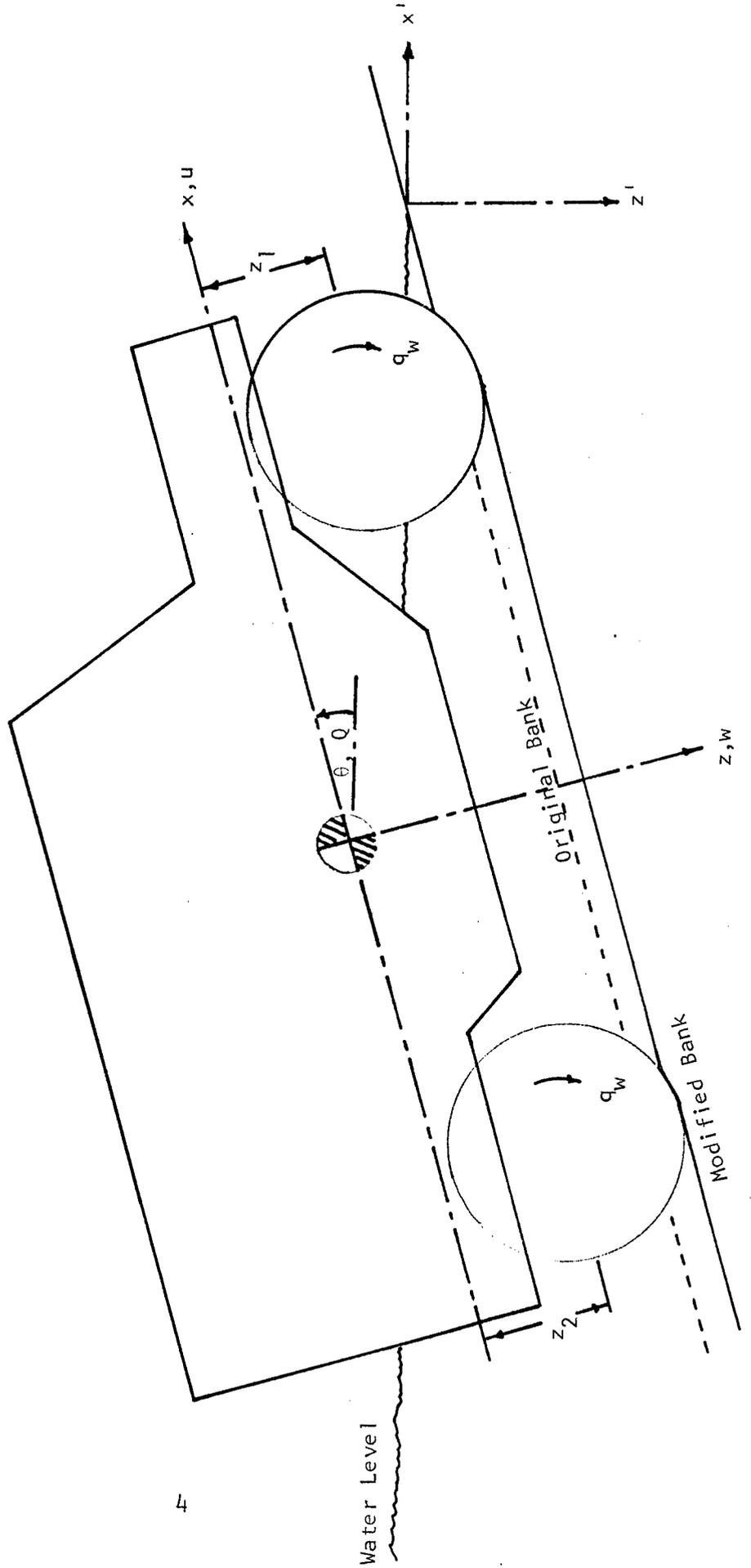
FIGURE 2. WHEEL AND SUSPENSION SCHEMATIC
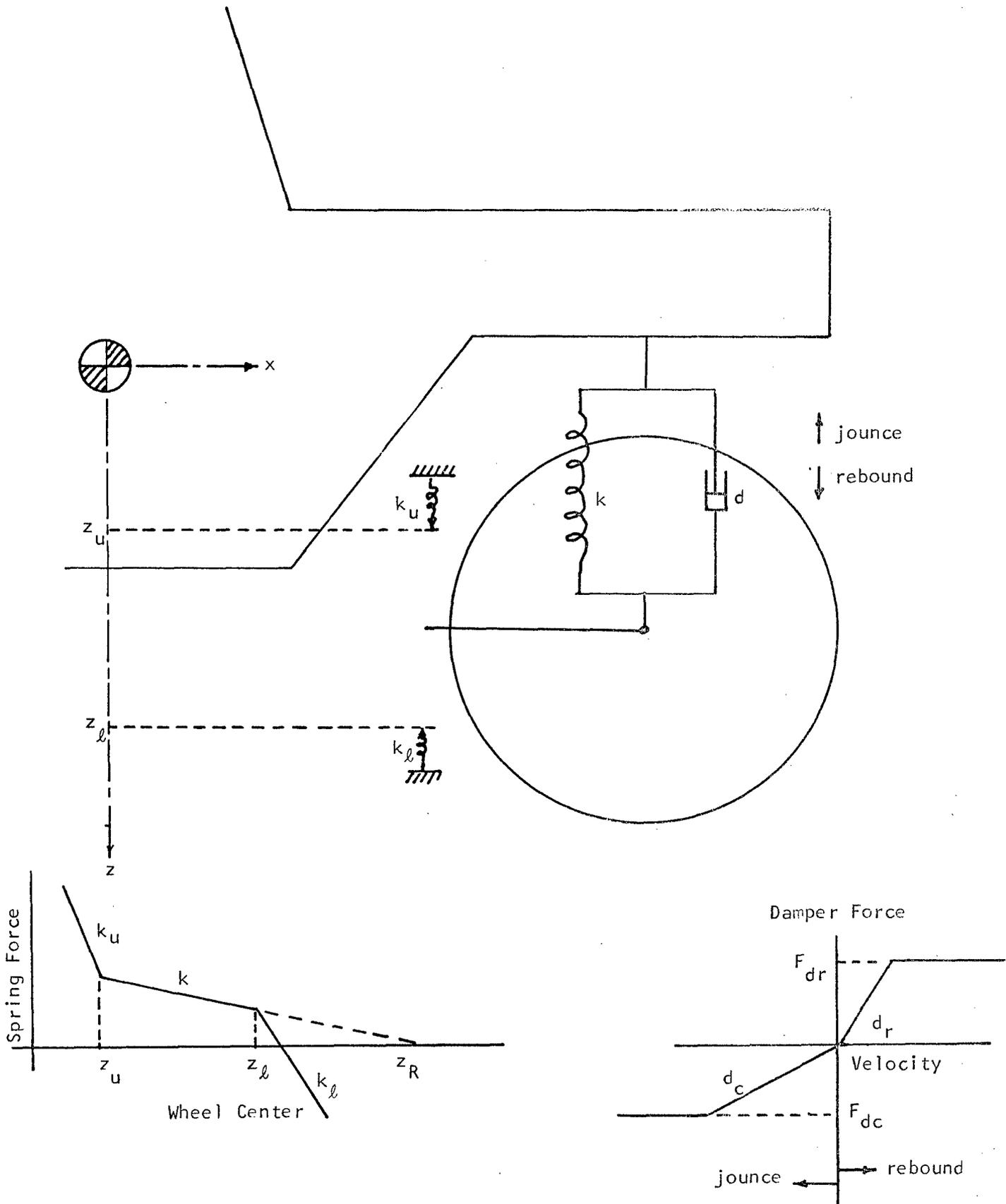
The drive train dynamics are governed by a curve relating engine RPM to torque at full throttle. The transmission is allowed up to nine different gear ratios. A single overall final drive ratio is assumed.

The Driver

The "driver model" currently assumes full-throttle at the lowest gear ratio possible for the required torque within the gear range specified at the commencement of each simulation run. The best driver strategy for egress is not yet known; hence it is expected that this portion of the model may eventually undergo many substantial revisions.

The Bank

The bank is described by a table relating bank surface elevation and distance relative to the water/bank intersection (see Figure 3). Elevation and soil parameters may change anywhere along the bank.

The bank coordinates are used as the earth-fixed frame of reference; vehicle position is specified in bank coordinates. The origin of this reference frame is at the water bank intersection; the horizontal water surface is the negative x'-axis; the z'-axis is vertical, positive down. The bank contour is specified by a number of convenient points, P_i , (see Figure 3) from which an auxiliary program, BNKPRO.F4, described in Reference 5, constructs the detailed bank profile by fitting a cubic equation to four consecutive straddling points, with appropriate modifications near the end points.

Soil strength characteristics along the bank are specified by a set of x'-coordinates (S_i in Figure 3). The region immediately to the left of each boundary point, S_i , is assumed to have homogeneous soil characteristics as specified by the land locomotion soil value system parameters. The particular manner in which they are used here is given by Miszklevitz.[6]
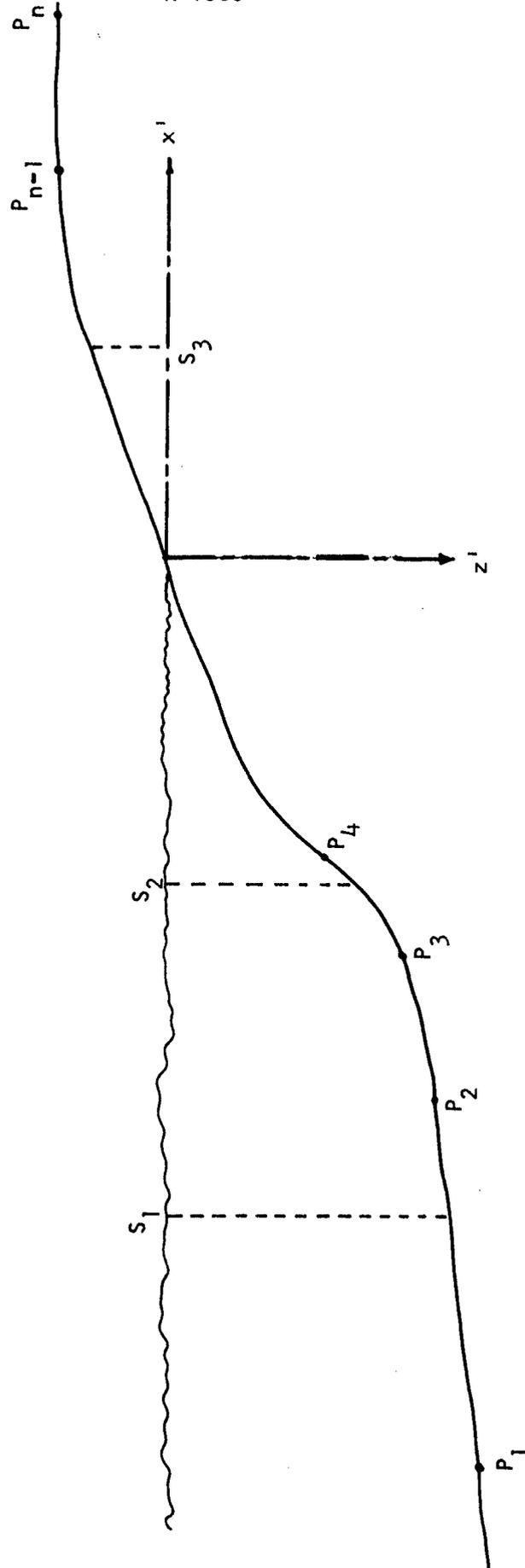
FIGURE 3. TYPICAL BANK PROFILE:
P_i ARE BANK PROFILE DATA POINTS;
S_i ARE BOUNDARIES BETWEEN HOMOGENEOUS SOIL REGIONS.

III. EQUATIONS

The state variables of the vehicular equations of motion are both the position and the velocities of the various vehicular components. Simplification of calculation is achieved by writing the differential equations of motion in the vehicle-based coordinate system shown in Figure 1 and:

1. Calculating the unbalanced forces resulting from the velocities and positions of each vehicular component,

2. Converting the unbalanced forces of Step 1 into resultant accelerations,

3. Integrating the appropriate accelerations of Step 2 and velocities of Step 1 to achieve new velocity and positional data,

4. Converting the new vehicular coordinate positions and velocities of Step 3 to earth-fixed coordinates,

5. Repeating the cycle by returning to Step 1 using the velocities and positions calculated in Step 4.

The fact that individual accelerations and forces are not calculated from a balance of forces means that no equilibrium analysis is employed. For example, traction at each wheel is not computed by calculating the net DBP required to overcome various resistances and allocating DBP to the various wheels by some method. Rather, individual wheel unbalances and interferences with, say, the soil are used to calculate forces and accelerations which, when converted to actual motions, will redress the unbalances. This general approach will be given explicit form in this section.

Forces governing vehicular and component motion result from the following convenient, though not mutually exclusive, categorization:

8

o soil/wheel compaction and shear

o water buoyancy

o viscous drag

o drive train thrust

o springs and dampers

o gravity

Actually, the only two sources of forces are gravity and the energy stored in the fuel which generates the drive train thrust. However, for convenience, the results of their application may be categorized as described above, if care is taken not to include a particular force under more than one category. The equations describing these forces in the vehicular coordinate system are presented below.

Soil-Wheel Interactions

The soil-wheel model employed here has been reported in detail by Miszklevitz.[6] Only a brief outline of this approach, along with the resulting equations, will be given here.

The major forces resulting from the soil-wheel interactions are the lift (or support) forces, primarily as a result of soil compaction due to sinkage resistance and the driving forces, primarily the result of soil shear due to the rotation of the wheel caused by drive train torque. In addition, the driving shear force also has a lift component and the compaction gives rise to a drag.

Due to the simplification of the vehicle suspension (motion of the wheel in the z-direction only) the pitch moments about the vehicle CG generated by the four forces mentioned above are treated somewhat differently depending on the coordinate direction in which they occur. Forces on the wheel in the z-direction result in motion of the wheel relative to the body. This relative motion results in suspension forces which are applied to the body at suspension attachment locations. Thus no pitch torques or heave forces resulting from soil-wheel z-direction forces are applied to the body directly; they will eventually appear as suspension forces and moments on the body. However, no relative x-direction motion between the

wheel and the body is allowed; therefore, soil-wheel x-direction forces give rise to pitch torques and surge forces on the body directly. The moment arms of these soil-inspired pitch torques are the z-distances from the CG of the body to the location in the soil-wheel contact patch where the soil forces are generated (see Figure 4).

FIGURE 4. SCHEMATIC SHOWING
SOIL-GENERATED FORCES AND MOMENTS.

At any instant in time, the wheel under consideration has a position relative to the bank which may or may not cause soil-wheel interference. If there is no interference, there are no soil-wheel forces. Interference is detected by calculating the z'-coordinate of many locations on the wheel circumference and comparing that with the corresponding z'-coordinates of the bank. When interference is detected, the locations of entry and exit interference with the original and current bank contours are determined and expressed as angles of the wheel relative to the horizontal (see Figure 5).
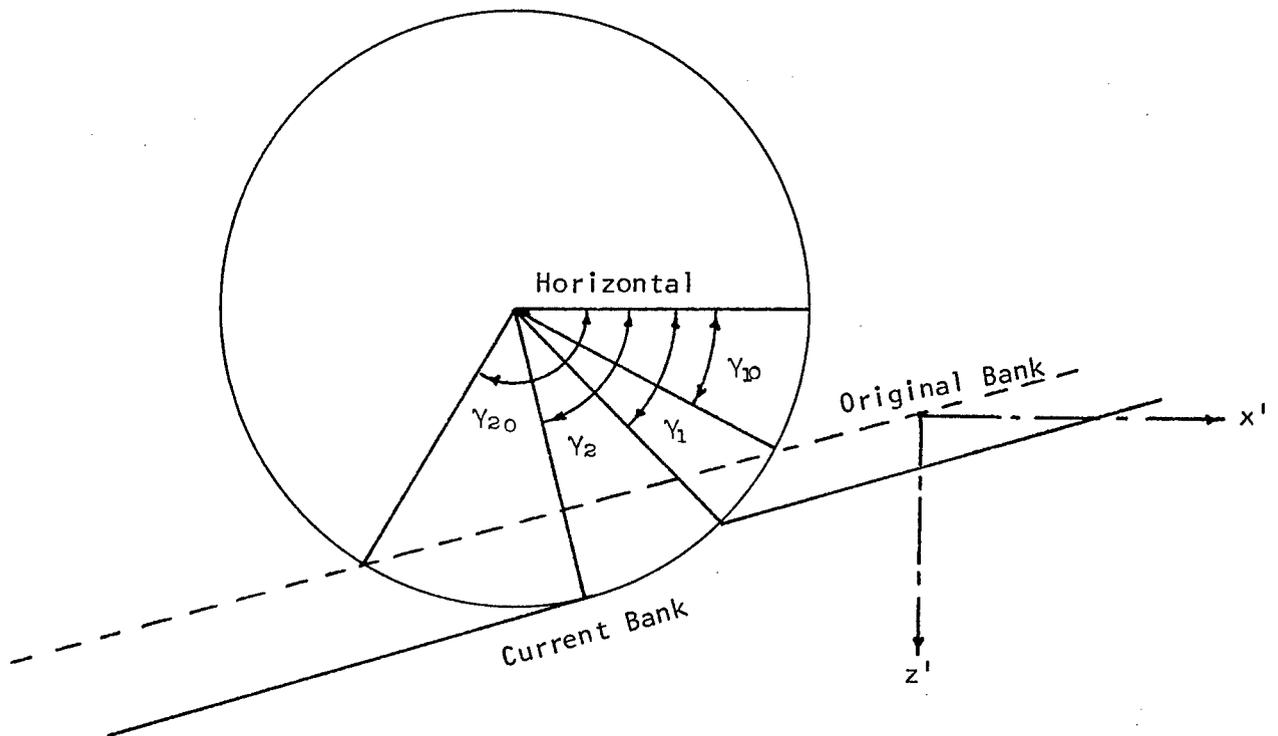

FIGURE 5. SCHEMATIC DEFINING SOIL-WHEEL
ENTRY AND EXIT LOCATIONS.

The actual ground contact patch extends only from the entry point, Y_1, to the exit point, Y_2. If, however, the bank originally had a contour different from the current position, the soil has experienced some pre-compaction. Therefore, to calculate the soil forces on the wheel, the normal stress distribution is computed as if soil-wheel contact extended from Y_{10} to Y_2, but is integrated only from Y_1 to Y_2 to calculate total normal force. (See Figure 6.) Support for this method of calculating lift forces is found in Bekker[7] and elsewhere; the entire argument is presented in detail by Miszklevitz.[6]

The normal force developed in the contact patch depends primarily on the maximum sinkage and the stress distribution. Here a symmetric quadratic stress distribution was postulated, not because it is known to be true, but because the deviations from measured distributions are not great and the resulting normal stress equation can be analytically integrated. If σ_{max} is the maximum normal stress and Y is any angle between Y_{10} and Y_2, then the normal stress at Y is postulated to be given by

$$\sigma(Y) = AY^2 + BY + C \qquad (1)$$

where

$$A = \frac{4\sigma_{max}}{(Y_{10}-Y_2)\,(Y_2-Y_{10})}$$

$$B = -(Y_{10}+Y_2)A$$

$$C = Y_{10}Y_2A \qquad (2)$$

This results in a distribution shown in Figure 7. The maximum normal stress, σ_{max}, is calculated from Bekker's equation

$$\sigma_{max} = \left(\frac{k_c}{b} + k_\varphi\right) z_m^n , \qquad (3)$$
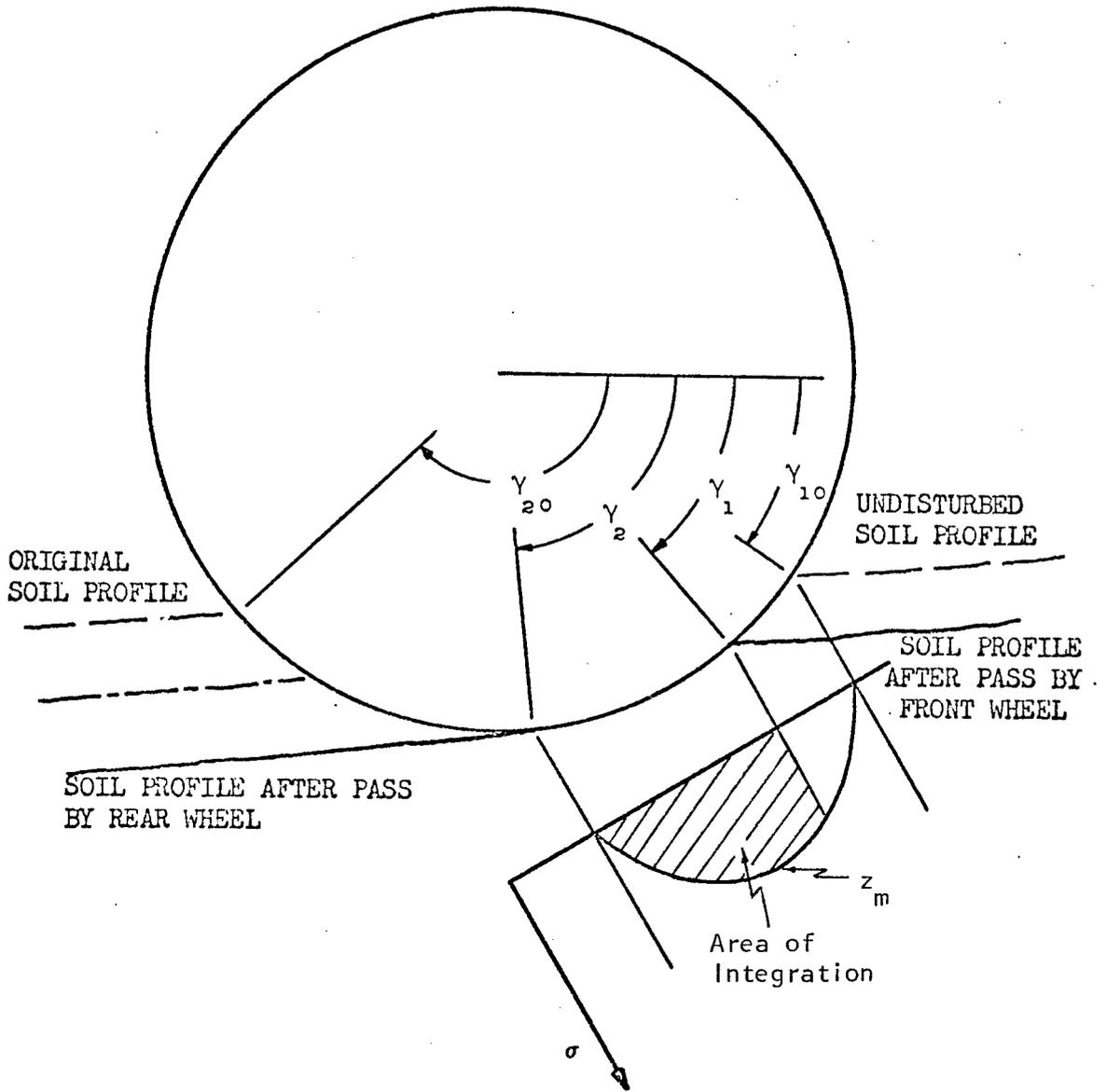
FIGURE 6. NORMAL STRESS DISTRIBUTION UNDER A REAR WHEEL
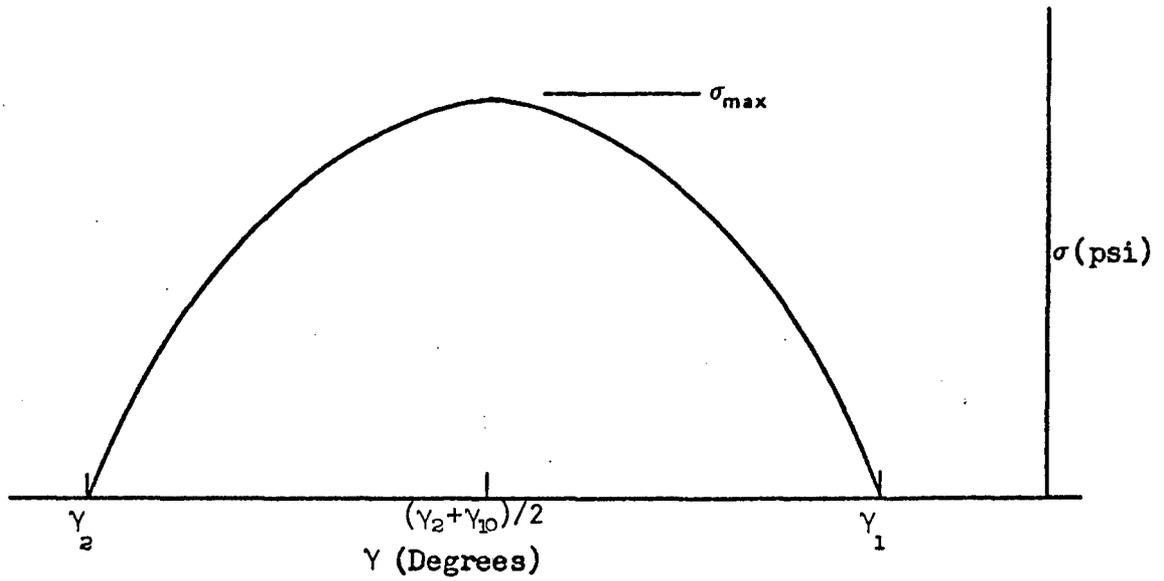
FIGURE 7. ASSUMED NORMAL STRESS DISTRIBUTION

$$d_1 = r \sin(\theta_G - \gamma_{1/2}) \qquad d_2 = r \sin(\theta_G - \gamma_{10})$$

$$z_m = d_1 - d_2$$
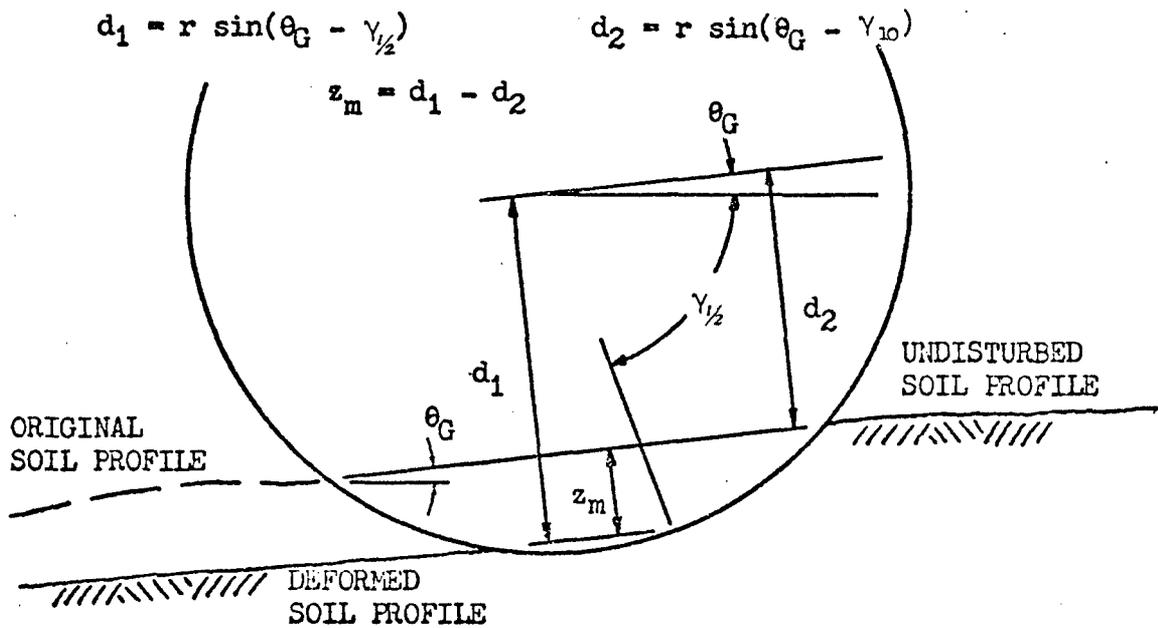
FIGURE 8. LOCAL GROUND SLOPE AND SINKAGE FOR A RIGID FRONT WHEEL

14

where z_m is the sinkage at the center of the contact patch (not necessarily the maximum sinkage, see Figure 6) which, for a wheel of radius r, is given by:

$$z_m = r[\sin(\theta_G - \frac{\lambda_{10} + \lambda_2}{2}) - \sin(\theta_G - \lambda_{10})] \qquad (4)$$

Here θ_G is the local ground slope, being the angle which the horizontal of the chord connecting the intersections of the wheel makes with the original bank surface, γ_{10} and γ_{20} (see Figure 8). Also k_c, k_φ and n in Equation (3) are Bekker's soil strength parameters.

The soil shear stress-strain distribution in the contact patch was proposed by Janosi and Hanamoto[8] as

$$\tau(\gamma) = (c + \sigma(\gamma) \tan\varphi) (1 - e^{-j/k}) \qquad (5)$$

Here, c and φ are the Coulomb soil shear strength parameters and j is the soil deformation, which is given (after Schuring and Belsdorf[9]) by

$$j = r[\gamma_1 - \gamma + (1-s) (\cos(\gamma - \theta_G) - \cos(\gamma_1 - \theta_G))] \qquad (6)$$

where

$$s = \frac{rq_w - u_G}{rq_w} = \text{the longitudinal slip of the wheel} \qquad (7)$$

q_w = the angular velocity of the wheel

u_G = the velocity component of the wheel center in the θ_G direction

The above equations for $\sigma(\gamma)$ and $\tau(\gamma)$ are used to assign normal and shear stresses to each point along the wheel contact patch between γ_1 and γ_2. These stresses are converted to vehicle coordinates and integrated over the contact patch to yield:

$$\text{Compression drag} = F_{x\sigma} = -\ br \int_{\gamma_2}^{\gamma_1} \sigma(\gamma)\ \cos(\gamma-\theta)\ d\gamma \tag{8}$$

$$\text{Compression lift} = F_{z\sigma} = br \int_{\gamma_2}^{\gamma_1} \sigma(\gamma)\ \sin(\gamma-\theta)\ d\gamma \tag{9}$$

$$\text{Shear thrust} = F_{x\tau} = -\ br \int_{\gamma_2}^{\gamma_1} \tau(\gamma)\ \sin(\gamma-\theta)\ d\gamma \tag{10}$$

$$\text{Shear lift} = F_{z\tau} = -\ br \int_{\gamma_2}^{\gamma_1} \tau(\gamma)\ \cos(\gamma-\theta)\ d\gamma \tag{11}$$

$$\text{Total shear moment on wheel} = T_{\tau} = br^2 \int_{\gamma_2}^{\gamma_1} \tau(\gamma)\ d\gamma \tag{12}$$

Compression drag moment about vehicle CG =

$$M_{x\sigma} = br \int_{\gamma_2}^{\gamma_1} (z_i + r\ \cos\alpha)\ \sigma(\gamma)\ \cos(\gamma-\theta)\ d\gamma \tag{13}$$

Shear thrust moment about vehicle CG =

$$M_{x\tau} = br \int_{\gamma_2}^{\gamma_1} (z_i + r\ \cos\alpha)\ \tau(\gamma)\ \sin(\gamma-\theta)\ d\gamma \tag{14}$$

But:

$$\alpha = \frac{\pi}{2} + \gamma - \theta$$

Therefore:

$$M_{x\sigma} = z_i F_{x\sigma} + br^2 \int_{\gamma_2}^{\gamma_1} \sigma(\gamma)\ \sin(\gamma-\theta)\ \cos(\gamma-\theta)\ d \tag{15}$$

$$M_{XT} = z_i F_{XT} + br^2 \int_{\gamma_2}^{\gamma_1} \tau(\gamma) \sin(\gamma-\theta) \cos(\gamma-\theta) \, d\gamma \qquad (16)$$

The total force parallel to the vehicle x-axis is given by:

$$F_{SX} = F_{XT} + F_{X\sigma} , \qquad (17)$$

and that parallel to the vehicle z-axis is:

$$F_{SZ} = F_{ZT} + F_{Z\sigma} \qquad (18)$$

Also:

$$M_{SX} = M_{X\sigma} + M_{XT} \qquad (19)$$

The equations for $F_{X\sigma}$, $F_{Z\sigma}$, and $M_{X\sigma}$ were integrated analytically by Miszklevitz.[6] The equations for F_{XT} , F_{ZT} and M_{XT} are not readily integratable analytically; so they are integrated numerically whenever needed. Details are presented in the Section IV describing the soil wheel interaction subroutine, SOILF.

Wheel Buoyancy

For purposes of the calculation of the buoyant forces on the wheels, it was assumed that the wheels were toroids of rectangular cross-section mounted on thin rims which do not displace a significant amount of water.

For a given z'-position of the center of the wheel, the area of the wheel torus under water multiplied by the wheel width would give the volume of water displaced. Multiplication of the displaced volume by the density of water yields the buoyant force on the wheel. Thus, for the disc defined in Figure 9:

$$\theta_w = \cos^{-1} (z'/r)$$

the area of wheel swept by $2\theta_w = \pi r^2 (\theta_w/\pi) = r^2\theta_w$

the area of triangle underwater $= \frac{1}{2} z' \, 2\sqrt{r^2-z'^2} = z' \sqrt{r^2-z'^2}$

Thus the total area submerged $= A_s = \pi r^2 - r^2\theta_w + z' \sqrt{r^2-z'^2}$ (20)
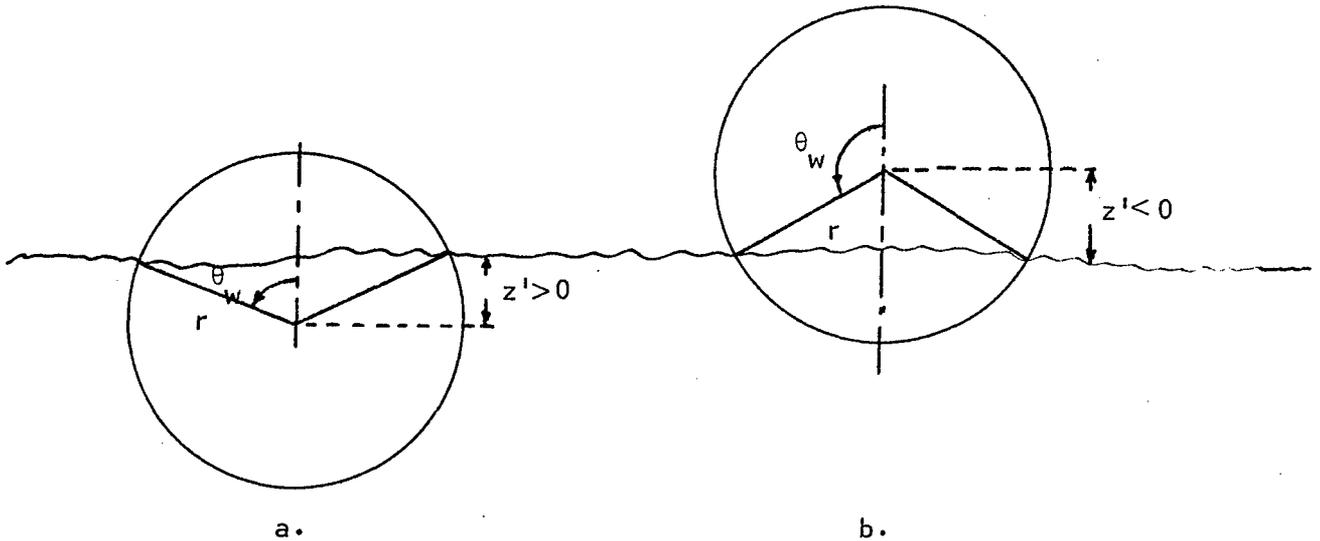
FIGURE 9. SIGNIFICANT VARIABLES IN THE WHEEL BUOYANCY CALCULATIONS

In Equation (20), r is either the radius of the wheel, r_w, or the radius of the rim, r_R.

Then, the wheel buoyant force is

$$F_b = \rho \, b(A_{sw} - A_{sR})$$ (21)

The line of action of the wheel buoyant force is always considered to be in the vertical (z'-negative) direction at the wheel center.

The calculations described above for both the wheel and rim buoyant forces are made for each wheel in the subroutine UPDATE, described in Section IV.

Wheel Rotational Drag

From a study by Ehrlich and Nuttall,[9] it is known that the hydraulic rotational drag on a spinning tires is sufficiently high to consume com-

pletely the torque derived from the M151 engine at approximately 25 mph.[*]
Data for the performance of an M151, with wheels fully submerged is given
in Table 1.

Figure 10 shows the estimated relationship between wheel rotational
drag, D_W (expressed in ft-lb), and wheel speed, q_W (expressed in rpm),
for the standard 7.00x16 NDCC tire mounted on the M151 1/4-ton truck. The
curve fitted to the data of Table 1 is:

$$D_W = a(q_W)^b \tag{22}$$

where:
$$a = .008123$$
$$b = 1.834$$

[*] The speedometer reading, not the linear speed of the vehicle.
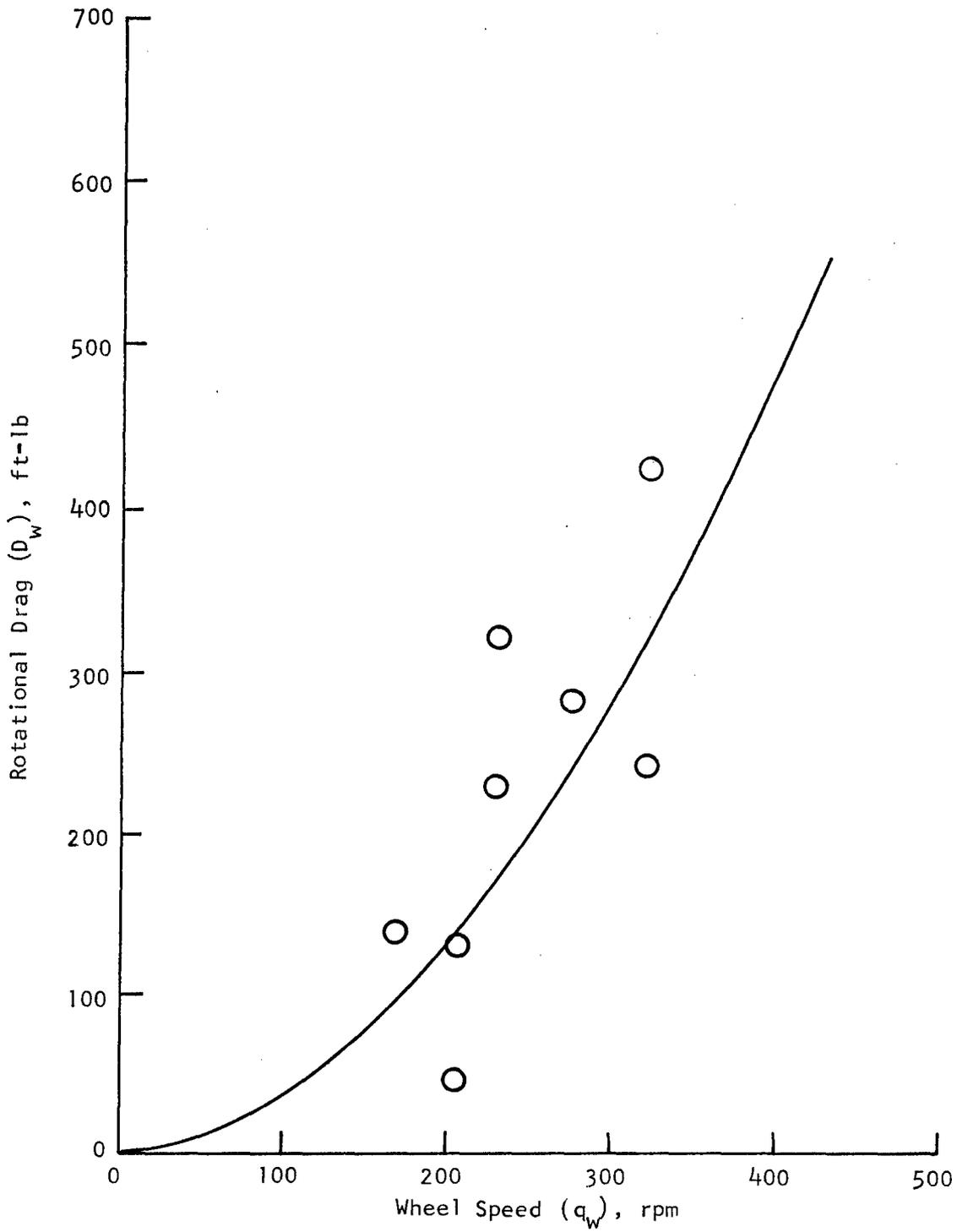
FIGURE 10. ESTIMATED RELATIONSHIP BETWEEN
WHEEL ROTATIONAL DRAG AND WHEEL SPEED,
7.00×16 NDCC TIRE FULLY SUBMERGED.

Table 1

MEASURED AND DERIVED PERFORMANCE OF
M151 WITH SUBMERGED WHEELS

Drive/Gear*	Maximum* Achievable Wheel Speed (rpm)	Equivalent* Engine Speed (rpm)	Estimated* Delivered Horsepower (hp)	Engine Torque (ft-lb)	Total Wheel Torque (ft-lb)	Torque (drag) per wheel (ft-lb)
2 wheel 1/1	208	6150	11	9.4	260.	130.
/2	324	5340	32	31.5	487.	244.
/3	324	2800	56	105.	854.	427.
/4	278	1440	32	117.	567.	284.
4 wheel 1/1	208	6150	11	9.4	260.	45.
/2	232	3820	61	83.9	1300.	324.
/3	232	2100	45	113.	915.	229.
/4	174	900	20	117.	567.	142.

*From Ehrlich and Nuttall[9].

If q_w is expressed in radians per second, a = 6.112 for Equation (22). This relationship is currently in the simulation in the subroutine UPDATE, described in Section IV. A change to other size wheels and tires may require a change to the program.

Driving Forces

For the purposes of this simulation, it is assumed that all wheels are rigidly connected to the drive train with no differential between adjacent wheels or between front and rear axles; the vehicle has a mechanical transmission; all final drive ratios are assumed equal; and the throttle is assumed fully open. The parameters describing such a drive train are:

o   the plot of engine RPM vs. torque at wide open throttle.

o   the number of gears, N_G , in the transmission and the ratio of each gear, G_i i = 1, ..., N_G .

o   the final drive ratio, G_F , which includes all gearing from the transmission to the wheels.

o   the efficiency of the transmission gears, η_G , and the final drive gear train, η_F .

o   the engine speed, S_R , at or below which the next lower gear is selected by the driver while decelerating.

o   the engine speed, U_R , above which the next higher gear is selected by the driver while accelerating.

Given the wheel speed, q_w , the engine speed is calculated for each transmission gear setting by:

$$E_{Ri} = G_i \, G_F \, q_w \quad \text{for } i = 1, \ldots, N_G \tag{23}$$

The lowest value of i for which $S_R < E_{Ri} \leq U_R$ is the selected gear ratio. For that gear the engine torque, T_E , at the engine speed, E_{Ri} , is calculated by interpolation from the table relating engine speed to engine torque at wide open throttle. The torque available to the wheels, T_w , is then calculated by:

$$T_W = T_E \, G_i \, \eta_G \, G_F \, \eta_F \tag{24}$$

These calculations are done in the subroutine UPDATE, described in Section IV.

Suspension Forces

Figure 2 defines the parameters of the suspension. Since the simulation is restricted to the vertical plane, the complicated suspension motions resulting in lateral side slip, camber and track variations are not included here. Wheel base variations were considered negligible.

These considerations led to simple wheel motions restricted to be only in heave (parallel to the vehicle z-direction). A no-load spring extension distance, z_R, is postulated which allows spring forces, S_p, to be calculated by

$$S_p = (z_R - z) \, k \quad \text{for} \quad z_u \leq z \leq z_\ell$$

$$S_p = (z_R - z_u) \, k + (z_u - z) \, k_u \quad \text{for } z < z_u$$

$$S_p = (z_R - z_\ell) \, k - (z - z_\ell) \, k_\ell \quad \text{for } z_\ell < z \tag{25}$$

The convention used here is that the suspension forces which act to separate the wheel from the body are positive.

Damper forces depend on the vertical velocity of the wheel, $\dot{z}$, and always oppose the motion of the wheel. Most hydraulic shock absorbers are constructed to give lower damping rates for compression (upward movement) than for rebound. In the current model there is provision for one damping rate, d_c, for negative values of $\dot{z}$ and another, d_r, for positive values. Furthermore, hydraulic shock absorbers have "blow off" characteristics; that is, they are capable of delivering forces only up to a given maximum value, F_d, usually different in each direction, F_{dc} and F_{dr}. Thus, the suspension forces S_d due to hydraulic dampers are:

$$S_d = \text{maximum} \{d_c \dot{z}, -F_{dc}\} \quad \text{for} \quad \dot{z} < 0$$

$$S_d = \text{minimum} \{d_r \dot{z}, F_{dr}\} \quad \text{for} \quad z \geq 0 \qquad (26)$$

The total suspension force is given by

$$D = S_p - S_d \qquad (27)$$

The above calculations are included in the subroutine UPDATE, described in Section IV.

Body Buoyant Forces

For purposes of buoyant force and center of buoyancy calculations, the body is divided (in the vertical plane) into rectangular boxes whose sides are parallel to the vehicle (x-z) coordinate axis. Each corner of each box are specified by one x- and one z-coordinate. The box is assumed centered along the y-axis and is assigned only a width, w_{Bi}.

The equation of the waterline in the vehicle coordinates is given by

$$z = s_w x + z_w \qquad (28)$$

where: the slope of water line with respect to the vehicle is

$$s_w = \tan \theta$$

the z-intercept of waterline with the vehicle coordinate is

$$z_w = -z'_{CG}/\cos \theta$$

The pitch angle θ, is restricted to be between $-\frac{\pi}{2}$ and $\frac{\pi}{2}$. The simulation ends if θ goes out of that range, since the vehicle has experienced a capsize.

Required for the calculations of the center of buoyancy are the equations which locate the centroid of a triangle, given the x- and z-coordinates of each apex. Thus, if the triangle has coordinates given in Figure 11, the centroid, c , has coordinates

$$\left(\frac{x_1 + x_2 + x_3}{3}, \quad \frac{z_1 + z_2 + z_3}{3} \right)$$

24

(x_3, z_3)

$(\frac{x_2+x_3}{2}, \frac{z_2+z_3}{2})$

$(\frac{x_1+x_3}{2}, \frac{z_1+z_3}{2})$

(x_2, z_2)

(x_1, z_1)
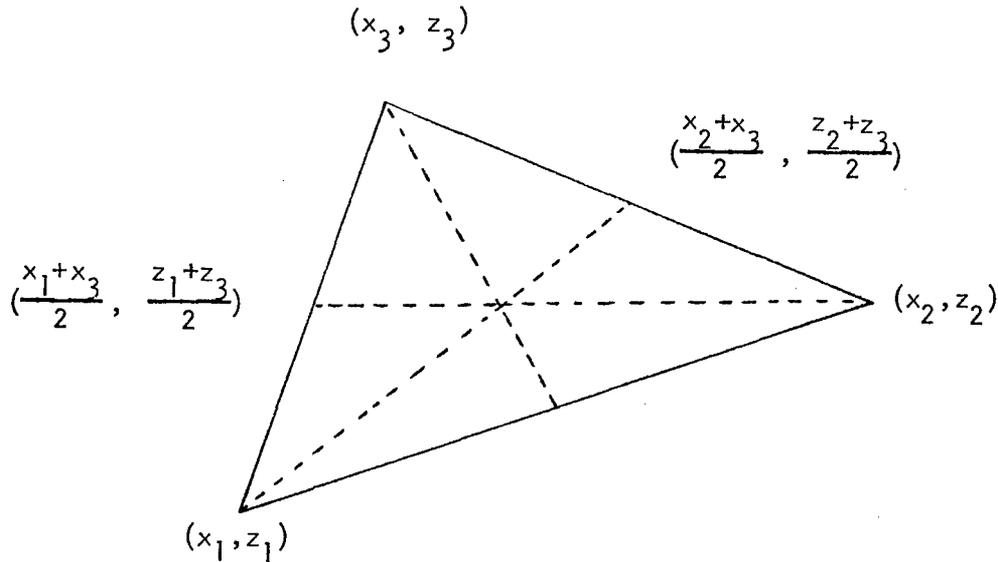
FIGURE 11. CENTROID OF TRIANGLE

In general, the buoyancy is calculated for each box by calculating the area of the box below the waterline, then multiplying by the width of the box and the density of water. The center of buoyancy is the centroid of the area under water. The line of action of the buoyant force is in the vertical upward (negative z') direction through the centroid.

Given the vehicle location, x'_{CG} and z'_{CG}, and the attitude, θ, the z'-coordinates of each of the box corners, z'_{Bj}, can be calculated by:

$$z'_{Bj} = z'_{CG} - x_{Bj} \sin \theta + z_{Bj} \cos \theta \quad j = 1,2,3,4 \qquad (29)$$

Here the subscripts are coded as:

subscript	corner of box
$j = 1$	lower front
$j = 2$	lower rear
$j = 3$	upper front
$j = 4$	upper rear

The values of z'_{Bj} are then compared to the water level (always at z' = 0) and the various possible positions of the box are categorized into the following cases:

25

Case 0. Box entirely out of water:

F_B = the force of buoyancy = 0

x_{FB} = the x-coordinate of the centroid = undefined

z_{FB} = the z-coordinate of the centroid = undefined   (30)

Case 1. Only the lower front corner (j = 1) under water (see Figure 12):

If the pitch angle, $|\theta|$, is less than .01, it is assumed that the entire box is out of the water and the calculations of Case 0 are performed.

4

2

3

A

z

B

x

1 (x_{B1}, z_{B1})

FIGURE 12. BUOYANCY CALCULATION, CASE 1

For $|\theta| \geq .01$, the coordinates of A are (x_A, z_{B1}) where $x_A = \dfrac{z_{B1} - z_w}{s_w}$, and the coordinates of B are (x_{B1}, z_B) where $z_B = x_{B1} s_w + s_w$.

The area submerged is

$$A_s = \frac{1}{2} (x_{B1} - x_A)(z_{B1} - z_B);$$

the force of buoyancy is

$$F_B = \rho A_s w_B ;$$ (31)

26

and the centroid is located at

$$x_{FB} = \frac{2x_{B1} + x_A}{3}$$

$$z_{FB} = \frac{2z_{B1} + z_B}{3} \qquad\qquad (31 \text{ cont'd})$$

Case 2. Only the lower rear corner (j = 2) is under water (see Figure 13):

If $|\theta| \le .01$, it is assumed the entire box is out of the water and the calculations of Case 0 are performed.
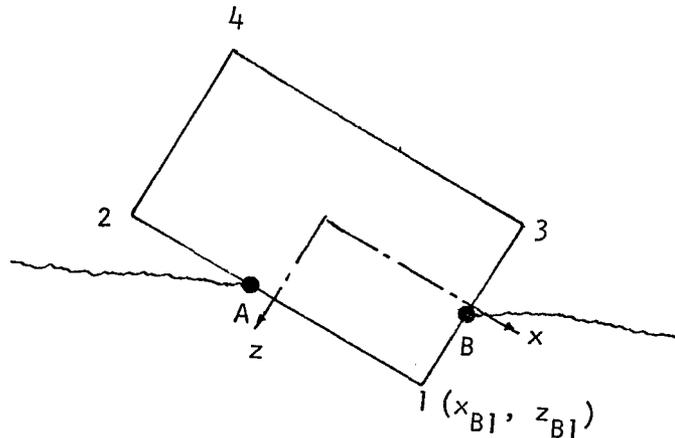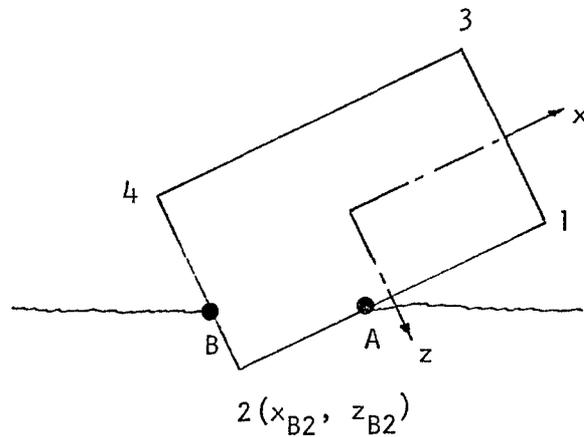

FIGURE 13. BUOYANCY CALCULATION, CASE 2

For $|\theta| \ge .01$, the coordinates of A are (x_A, z_{B2}) where $x_A = \dfrac{z_{B2} - z_w}{s_w}$ and the coordinates of B are (x_{B2}, z_B) where $z_B = x_{B2} s_w + z_w$.

The area submerged is

$$A_s = \frac{1}{2} (z_{B2} - z_B) (x_A - x_{B2}) \; ;$$

the force of buoyancy is

$$F_B = \rho \, A_s \, w_B \; ;$$

and the centroid is located at

$$x_{FB} = \frac{2x_{B2} + x_A}{3}$$

(32)

$$z_{FB} = \frac{2z_{B2} + z_B}{3}$$

Case 3. Both lower corners ($j = 1$, $j = 2$) only are under water (see Figure 14):
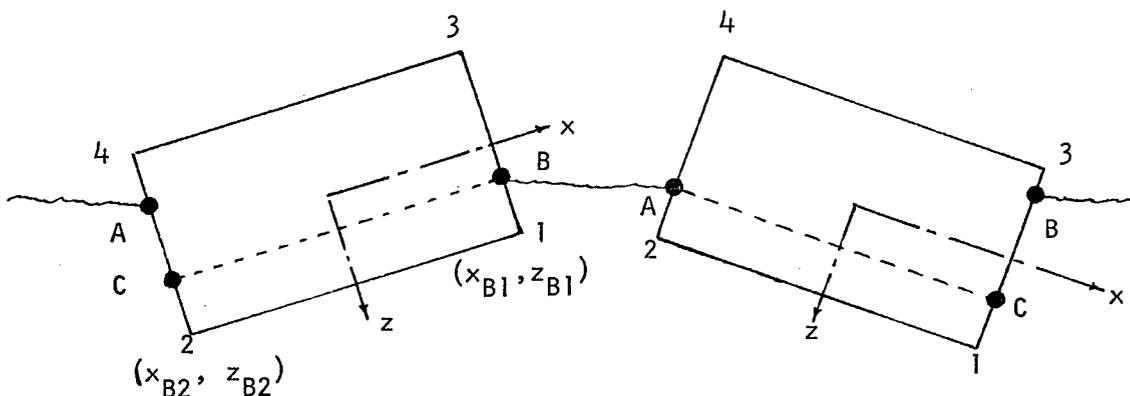
FIGURE 14. BUOYANCY CALCULATION, CASE 3

The coordinates of A are (x_{B2}, z_A) where $z_A = x_{B2} \, s_w + z_w$, the coordinates of B are (x_{B1}, z_B) where $z_B = x_{B1} \, s_w + z_w$, and the coordinates of C are (x_C, z_C) where

$$x_C = x_{B2}, \; z_C = z_B \quad \text{if} \quad z_B \geq z_A$$

$$x_C = x_{B1}, \; z_C = z_A \quad \text{if} \quad z_B < z_A$$

Let
$$z_D = z_A \quad \text{for} \quad z_B \geq z_A \quad ,$$

$$z_D = z_B \quad \text{for} \quad z_B < z_A \quad ,$$

A_T = area of triangle, ABC ,

A_R = area of rectangle 12CB for $z_B \geq z_A$, or 12AC for $z_B < z_A$,

$\ell = x_{B1} - x_{B2}$

Then

$$A_T = \frac{1}{2} \ell (z_C - z_D)$$

and the centroids of the area A_T are

$$\bar{x}_T = \frac{x_{B1} + x_C + x_{B2}}{3}$$

$$\bar{z}_T = \frac{z_A + z_B + z_C}{3}$$

Also

$$A_R = \ell (z_{B2} - z_C)$$

and the centroids of the area A_R are

$$\bar{x}_R = \frac{x_{B1} + x_{B2}}{2}$$

$$\bar{z}_R = \frac{z_{B2} + z_C}{2}$$

The submerged area is then

$$A_s = A_T + A_r \quad ;$$

the force of buoyancy is

$$F_B = \rho A_s w_B \; ;$$

and the centroid of the submerged area is located at

$$x_{FB} = \frac{\bar{x}_T A_T + \bar{x}_R A_R}{A_s} \qquad (33)$$

$$z_{FB} = \frac{\bar{z}_T A_T + \bar{z}_R A_R}{A_s}$$

Case 4. Both front corners ($j = 1$, $j = 3$) only are submerged (see Figure 15):
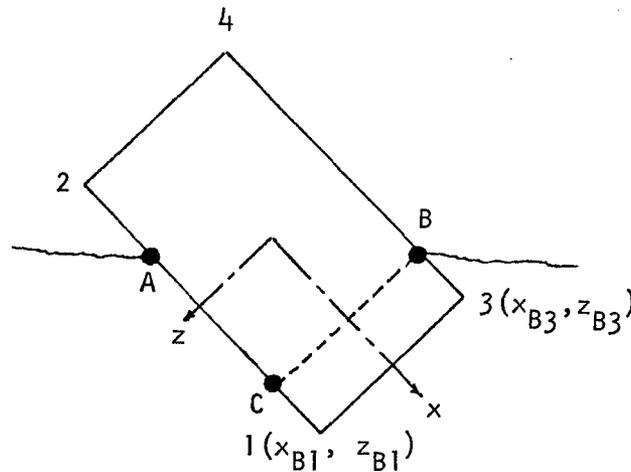
FIGURE 15. BUOYANCY CALCULATION, CASE 4

Since θ is never less than $-\frac{\pi}{2}$, C can be assigned without ambiguity and the coordinates of A, B and C are (x_A, z_{B1}), (x_B, z_{B3}) and (x_C, z_{B1}), respectively, and:

$$x_A = \frac{z_{B1} - z_w}{s_w}$$

$$x_B = \frac{z_{B3} - z_w}{s_w}$$

$$x_C = x_B$$

30

With the symbols as defined in Case 3, and $h = z_{B1} - z_{B3}$:

$$A_T = \frac{1}{2} h (x_C - x_A)$$

$$\bar{x}_T = \frac{x_A + x_B + x_C}{3}$$

$$\bar{z}_T = \frac{2z_{B1} + z_{B3}}{3}$$

$$A_R = h(x_{B1} - x_C)$$

$$\bar{x}_R = \frac{x_{B1} + x_C}{2}$$

$$\bar{z}_R = \frac{z_{B1} + z_{B3}}{2}$$

Then the submerged area is

$$A_s = A_T + A_R \quad ;$$

the force of buoyancy is

$$F_B = \rho A_s w_B \quad ;$$

$$x_{FB} = \frac{\bar{x}_T A_T + \bar{x}_R A_R}{A_s} \tag{34}$$

$$z_{FB} = \frac{\bar{z}_T A_T + \bar{z}_R A_R}{A_s}$$

Case 5. Both rear corners ($j = 2$, $j = 4$) only are submerged (see Figure 16)
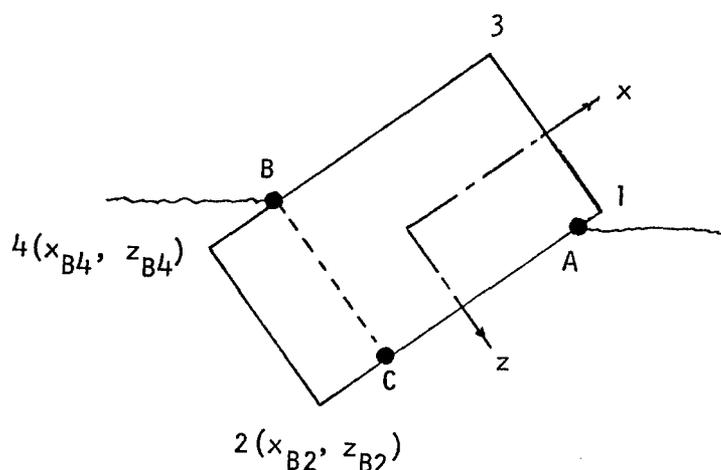
FIGURE 16. BUOYANCY CALCULATION, CASE 5

Again, since θ is never greater than $\frac{\pi}{2}$, C can be assigned without ambiguity and the coordinates of A, B and C are (x_A, z_{B2}), (x_B, z_{B4}), and (x_C, z_{B2}), respectively, and:

$$x_A = \frac{z_{B2} - z_w}{S_w}$$

$$x_B = \frac{z_{B4} - z_w}{S_w}$$

$$x_C = x_B$$

With the symbols defined in Cases 3 and 4,

$$A_T = \frac{1}{2} h(x_A - x_C)$$

$$\bar{x}_T = \frac{x_A + x_B + x_C}{3}$$

$$\bar{z}_T = \frac{2z_{B2} + z_{B4}}{3}$$

$$A_R = h(x_C - x_{B2})$$

$$\bar{x}_R = \frac{x_C + x_{B2}}{2}$$

$$\bar{z}_R = \frac{z_{B2} + z_{B4}}{2}$$

Then

$$A_s = A_T + A_R$$

$$F_B = \rho A_s w_B$$

$$x_{FB} = \frac{\bar{x}_T A_T + \bar{x}_R A_R}{A_s}$$

$$z_{FB} = \frac{\bar{z}_T A_T + \bar{z}_R A_R}{A_s}$$

(35)

Case 6. All but upper front corner are submerged (see Figure 17).

If $|\theta| < .01$, the entire box is assumed submerged and the calculations of case 8 are performed.
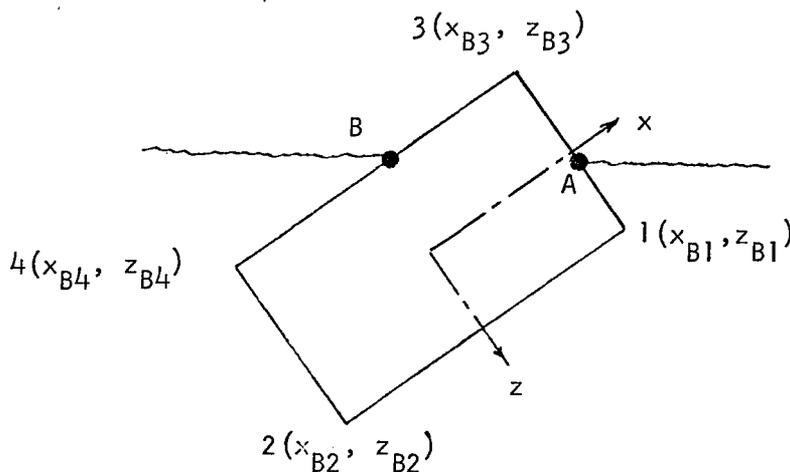
FIGURE 17. BUOYANCY CALCULATION, CASE 6

If $|\theta| \geq .01$, the coordinates of A and B are (x_{B3}, z_A) and (x_B, z_{B3}), respectively, where $z_A = x_{B3} s_w + z_w$ and $x_B = \frac{z_{B3} - z_w}{s_w}$.

The symbols are as defined before, and

$$A_T = \frac{1}{2} (z_A - z_{B3})(x_{B3} - x_B)$$

$$\bar{x}_T = \frac{2x_{B3} + x_B}{3}$$

$$\bar{z}_T = \frac{2z_{B3} + z_A}{3}$$

Then $A_s = \ell h - A_T$ and

$$F_B = \rho A_s w_B$$

$$x_{FB} = \frac{\frac{1}{2}(x_{B1} + x_{B2})\ell h - \bar{x}_T A_T}{A_s} \tag{36}$$

$$z_{FB} = \frac{\frac{1}{2}(z_{B1} + z_{B3})\ell h - \bar{z}_T A_T}{A_s}$$

Case 7. All but upper rear corner are submerged (see Figure 18).

If $|\theta| < .01$, it is assumed that the entire box is under water and the results are as in Case 8, below.
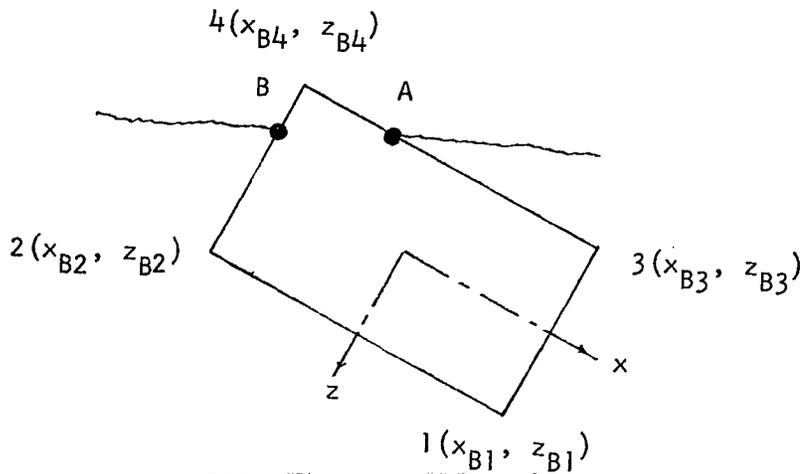
FIGURE 18. BUOYANCY CALCULATION, CASE 7

If $|\theta| \geq .01$, the coordinates of A and B are (x_A, z_{B4}) and (x_{B4}, z_B), respectively, where $x_A = \dfrac{z_{B4} - z_w}{s_w}$ and $z_B = x_{B4} s_w + z_w$.

The symbols are as defined before, and

$$A_T = \frac{1}{2} (z_B - z_{B4})(x_A - x_{B4})$$

$$\bar{x}_T = \frac{2x_{B4} + x_A}{3}$$

$$\bar{z}_T = \frac{2z_{B4} + z_B}{3}$$

Then $A_s = \ell h - A_T$ and

$$F_B = \rho A_s w_B$$

$$x_{FB} = \frac{\frac{1}{2}(x_{B1} + x_{B2})\ell h - \bar{x}_T A_T}{A_s} \qquad (37)$$

$$z_{FB} = \frac{\frac{1}{2}(z_{B1} + z_{B3})\ell h - \bar{z}_T A_T}{A_s}$$

Case 8. Entire box submerged.

In this case, with the symbols defined as before,

$$F_B = \rho \ell h \, w_B$$

$$x_{FB} = \frac{1}{2}(x_{B1} + x_{B2}) \qquad (38)$$

$$z_{FB} = \frac{1}{2}(z_{B1} + z_{B3})$$

Both the determination of which case exists, and the calculations, are coded into a subroutine called BBOX, described in Section IV.

Equations of Motions

The equations of motion used here are a restriction of those derived by Etkin[11] for six degrees-of-freedom, body centered coordinates. The restrictions are those that allow only vertical plane motion. This means that surge, roll and yaw motions are assumed constantly zero.

Let n_A be the number of axles, and n_B be the number of body boxes. To simplify notation in this section, the use of the subscript i after Σ implies summation over all axles; i.e., $i = 1,...,n_A$, and the use of the subscript j implies summation over all body boxes, i.e., $j = 1,...,n_B$.

The surge degree-of-freedom of the sprung mass is governed by the equation

$$M_s(\dot{u}+wQ) = 2[\Sigma F_{sxi}-\sin\theta \Sigma F_{bi}] - [W+\Sigma F_{Bj}]\sin\theta - \Sigma M_{ui}a_{xi} \tag{39}$$

Here $M_{ui}a_{xi}$ is the force exerted on the body due to the acceleration of the ith axle in the x-direction and is given in this case (see Jurkat[12] for derivation) by

$$a_{xi} = \dot{u} + wQ + 2Q\dot{z}_i - x_iQ^2 + z_i\dot{Q} \tag{40}$$

Then, substituting a_{xi} into Equation (39) and solving for the terms involving derivatives

$$M\dot{u}+(\Sigma M_{ui}z_i)\dot{Q}+2Q\Sigma M_{ui}\dot{z}_i = -wQM_s+2[\Sigma F_{sxi}-\sin\theta\Sigma F_{bi}] - [W+F_{Bj}]\sin\theta$$
$$- Q\Sigma M_{ui}(w-x_iQ) \tag{41}$$

Let F_x denote the right hand side of this equation, that is

$$F_x = -wQM_s+2[\Sigma F_{sxi}-\sin\theta \Sigma F_{bi}] - [W+\Sigma F_{Bj}]\sin\theta-Q\Sigma M_{ui}(w-x_iQ) \tag{42}$$

The heave degree of freedom is governed by a simpler equation since all z-axis motion of the unsprung masses results in spring and damper forces, not inertial forces directly on the sprung mass. Therefore, in heave,

$$M_s(\dot{w} - uQ) = -\Sigma D_i + (W_s + \Sigma F_{Bj}) \cos\theta \qquad (43)$$

Again, solving for the terms containing derivatives, and renaming the right-hand side F_z

$$M_s\dot{w} = M_s uQ - \Sigma D_i + (W_s + \Sigma F_{Bj})\cos\theta = F_z \qquad (44)$$

The pitch equation requires organization to maintain the reader's orientation. The "applied" moments are derived from the following:

- o suspension spring and damper forces
- o wheel-soil forces in the x-direction
- o weight of the wheels in the x-direction
- o buoyancy of the wheels in x-direction
- o buoyancy of the body boxes in all directions
- o driving torque on the wheels
- o tangential soil drag on the wheels
- o tangential hydrodynamic drag on the wheels
- o inertial reactions

The pitch equation of motion, with terms written in the above order, then becomes:

$$I_{ys}\dot{Q} = \Sigma D_i x_i + 2\Sigma M_{sxi} - \Sigma W_{ui} z_i \sin\theta$$
$$- 2\Sigma F_{bi} z_i \sin\theta - \Sigma F_{Bj} x_{FBj} \cos\theta - F_{Bj} z_{FB_j} \sin\theta$$
$$- T_w + \Sigma(T_{Ti} - D_{wi}) - \Sigma M_{ui} z_i a_{xi} \qquad (45)$$

After substituting a_{xi} from Equation (40) into Equation (45) and solving for those terms containing the derivatives (note the moments of inertia of the unsprung masses-- $\Sigma M_{ui} z_i^2 \dot{Q}$ -- add to $I_{ys}\dot{Q}$ to produce the total mass term $I_y \dot{Q}$) we obtain:

$$(\Sigma M_{ui}z_i)\dot{u} + I_y\dot{Q} - \Sigma(2QM_{ui}z_i)\dot{z}_i = \Sigma D_i x_i + 2\Sigma M_{sxi}$$

$$- \Sigma W_{ui}z_i \sin\theta - 2\Sigma F_{bi}z_i \sin\theta$$

$$- \Sigma F_{Bj}x_{FBj}\cos\theta - \Sigma F_{Bj}z_{FBj}\sin\theta + T_w$$

$$+ \Sigma(T_{Ti} - D_{wi}) - Q\,\Sigma M_{ui}z_i(w - x_i Q) \qquad (46)$$

Let the right hand side of Equation (46) be denoted by G_y.

The equation governing the rotational speed of the wheels is

$$I_w\dot{q}_w = T_w + 2\Sigma(T_{Ti} - D_{wi}) \qquad (47)$$

The equation governing the position of each wheel center relative to the vehicle is

$$M_{ui}\ddot{z}_i = W_{ui}\cos\theta + D_i + 2F_{szi} + 2F_{bi}\cos\theta \qquad (48)$$

Let the right hand side of Equation (48) be denoted by F_{zi}.

Required for the simulation are the position and velocity of the sprung-mass center of gravity in bank coordinates. This is found by calculating the velocity of the sprung-mass CG in bank coordinates from

$$u' = u\cos\theta + w\sin\theta \qquad (49)$$

$$w' = -u\sin\theta + w\cos\theta \qquad (50)$$

and integrating.

The equations for $\dot{q}_w$, u', and w' are uncoupled from the others and may be treated alone. The remaining equations are coupled and cannot be integrated until solved as a system for the derivative terms. To this end, we write them as a linear system as follows:

$$
\begin{pmatrix}
M & 0 & \overline{M}_u & \vline & 2QM_{u1} & 2QM_{u2} & \cdots & 2QM_{un_A} \\
0 & M_s & 0 & \vline & 0 & 0 & \cdots & 0 \\
\overline{M}_u & 0 & I_y & \vline & 2QM_{u1}z_1 & 2QMu_2z_2 & \cdots & 2QM_{un_A}z_{n_A} \\
\hline
0 & 0 & 0 & \vline & 1 & 0 & & 0 \\
0 & 0 & 0 & \vline & 0 & 1 & & 0 \\
\vdots & & & \vline & & & & \\
0 & 0 & 0 & \vline & 0 & 0 & & 1
\end{pmatrix}
\begin{pmatrix}
\dot{u} \\ \dot{w} \\ \dot{Q} \\ \dot{z}_1 \\ \dot{z}_2 \\ \vdots \\ \dot{z}_{n_A}
\end{pmatrix}
=
\begin{pmatrix}
F_x \\ F_z \\ G_y \\ z_{n_A+1} \\ z_{n_A+2} \\ \vdots \\ z_{2n_A}
\end{pmatrix}
\tag{51}
$$

Here $\overline{M}_u = \Sigma M_{ui}z_i$ and the convention of writing the wheel equation by letting

$$
\begin{aligned}
\dot{z}_i &= z_{n_A+i} \\
\dot{z}_{n_A+i} &= F_{zi}
\end{aligned}
\qquad \text{for} \quad i = 1,\ldots,n_A
\tag{52}
$$

was followed.

The left-most matrix of Equation (51) may be partitioned along the dashed lines. Therefore, if we define A, B, C and D as follows:

$$
A = \begin{pmatrix}
M & 0 & \overline{M}_u \\
0 & M_s & 0 \\
\overline{M}_u & 0 & I_y
\end{pmatrix}
$$

$$
B = \begin{pmatrix}
2QM_{u1} & 2QM_{u2} & \cdots & 2QM_{un_A} \\
0 & 0 & \cdots & 0 \\
2QM_{u1}z_1 & 2QMu_2z_2 & \cdots & 2QM_{un_A}z_{n_A}
\end{pmatrix}
$$

$$\tag{53}$$

$$C = (n_A \times 3) \text{ zero matrix} = 0_{n_A \times 3}$$

$$(53 \text{ cont'd})$$

$$D = n_A \times n_A \text{ identity matrix} = I_{n_A \times n_A}$$

Then the system of Equations (51) may be written as

$$J \begin{pmatrix} \dot{u} \\ \dot{w} \\ \dot{Q} \\ \dot{z}_i \\ \cdot \\ \cdot \\ \cdot \\ z_{n_A} \end{pmatrix} = \begin{pmatrix} F_x \\ F_z \\ G_y \\ z_{n_a+1} \\ \cdot \\ \cdot \\ \cdot \\ z_{2n_A} \end{pmatrix} \tag{54}$$

where

$$J = \begin{pmatrix} A & B \\ C & D \end{pmatrix} \tag{55}$$

The System (51) may then be solved by finding the inverse of J. If

$$J^{-1} = \begin{pmatrix} E & F \\ G & H \end{pmatrix} \tag{56}$$

then

$$E = A^{-1}$$

$$F = - A^{-1} B$$

$$G = 0_{n_A \times 3} \tag{57}$$

$$H = I_{n_A \times n_A}$$

This means that only the 3X3 matrix A needs to be inverted. Its inverse is given by

$$E = \frac{1}{\overline{M}} \begin{pmatrix} I_y & 0 & -\overline{M}_u \\ 0 & \overline{M}/M_s & 0 \\ -\overline{M}_u & 0 & M \end{pmatrix}$$ (58)

where $\overline{M} = MI_y - \overline{M}_u^2$. Then

$$F = -\frac{2Q}{\overline{M}} \begin{pmatrix} I_y M_{u1} - \overline{M}_u M_{u1} z_1 & \cdots & I_y M_{un_A} - \overline{M}_u M_{un_A} z_{n_A} \\ 0 & \cdots & 0 \\ M M_{u1} z_1 - M_{u1} \overline{M}_u & \cdots & M M_{un_A} z_{n_A} - M_{un_A} \overline{M}_u \end{pmatrix}$$ (59)

Multiplying the matrix J^{-1} thus defined by the vector on the right hand side of the system yields the following set of first order equations, separated by degrees of freedom:

$$\overline{M}\dot{u} = I_y F_x - \overline{M}_u G_y - 2Q\Sigma \, [M_{ui}(I_y - \overline{M}_u z_i) z_{n_A+1}]$$ (60)

$$M_s \dot{w} = F_z$$ (61)

$$\overline{M}\dot{Q} = -M_u F_x + M \, G_y - 2Q\Sigma \, [M_{ui}(Mz_i - \overline{M}_u) z_{n_A+i}]$$ (62)

$$\dot{z}_i = z_{n_A+1}$$ (63)

$$i = 1,2,\ldots,n_A$$

$$M_{ui} z_{n_A+1} = F_{zi}$$ (64)

These equations may now be integrated separately.

IV. SIMULATION

The simulation described by the previous equations is mechanized in a FORTRAN IV program written for the Digital Equipment Corporation PDP-10 computer located in the Stevens Institute of Technology Computer Center. The program, called EGRES3.F4 is run under the time-sharing monitor and loads into 13K of core. Required for the simulation, in addition to various subroutines built into the FORTRAN compiler, is the subroutine HPCG, part of the Scientific Subroutine Package (SSP)[12], assembled by IBM for their 360 FORTRAN compilers. This subroutine controls the simulation and performs the numerical integration of the equations of motion by a variable, multi-step fifth-order predictor-corrector.

Initially, the simulation is started by the subroutine INPUT that first reads the vehicle and bank parameters, which are stored in COMMON and then sets the initial values of the state variables and stores them in an array called Y. The derivatives of the state variables are then calculated and stored in an array called DY by a subroutine called UPDATE and various other subroutines called by UPDATE. The program HPCG then generates "new" values of the state variables for Y and calls on UPDATE to compute new values for DY as a result of tne new Y values. This cycle keeps repeating until the simulation is terminated. At appropriate times HPCG calls subroutine OUTPUT which writes the values of the state variables in Y and many others of interest onto a disk file for future printing. The subroutine hierarchy is given in Figure 19. The variables shown in Figure 19 are only the significant ones passed directly from subroutine to subroutine.
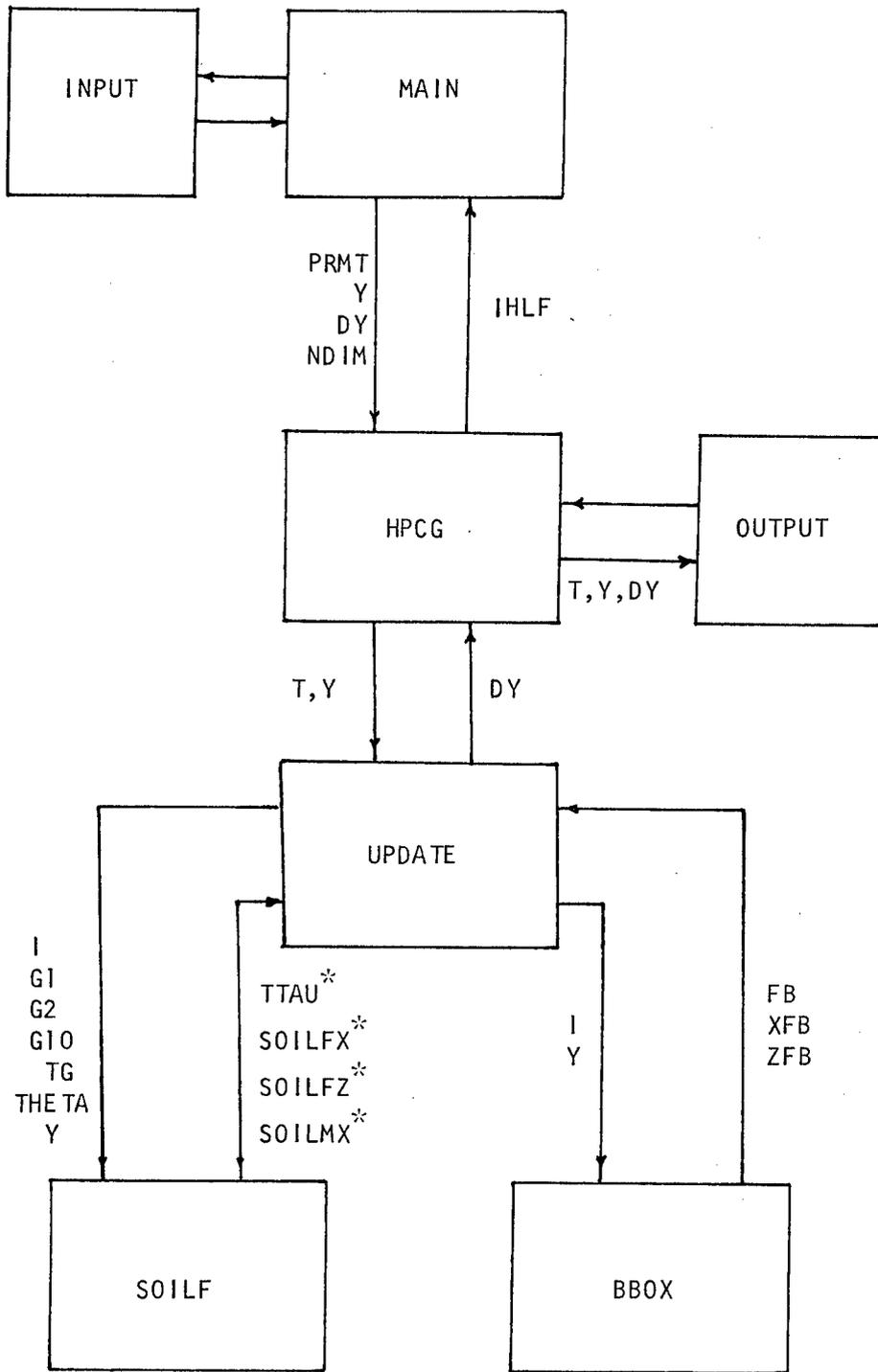
* Variables in common

FIGURE 19. ORGANIZATION OF EGRES3.F4

The storage scheme in Y is as follows:

$Y(1) = u =$ the velocity of the sprung mass CG in the vehicle x-direction (positive is forward)

$Y(2) = w =$ the velocity of the sprung mass CG in the vehicle z-direction (positive is down)

$Y(3) = Q =$ the vehicle pitch velocity (positive is nose up)

$Y(4) = q_w =$ the rotational velocity of the wheels (positive is clockwise-rotation, compatible with forward motion)

$Y(5) = x'_{CG} =$ the x'-coordinate of the sprung mass CG (positive is to right of the water's edge)

$Y(6) = z'_{CG} =$ the z'-coordinate of the sprung mass CG (positive is down)

$Y(7) = \theta =$ the pitch angle (positve is nose up)

$Y(7+i) = z_i =$ the z-distance from vehicle CG of the center of wheel i (positive is down)

$Y(7+n_A+i) = \dot{z}_i =$ the z-velocity of the center of wheel i (positive is down)

Here $i = 1,...,n_A$. Although COMMON contains room for $n_A = 8$, Y, DY and AUX are currently only DIMENSIONED large enough for two axles. Thus its size must be changed for vehicles with more than two axles.

EGRES3.F4 requires the availability, on device 21, of a file containing the vehicle parameters and a file containing the bank soil values and profile. These files are to be in the format described in Reference 5.

The following describes each of the program routines in more detail. It is suggested that the reader have before him the listing of the program and follow it while reading. This listing may be found in Reference 5.

MAIN Program

The MAIN program of EGRES3.F4 serves only to establish storage, to set various initializing values, to call INPUT, and then to turn over control of the simulation to HPCG. Control is not returned to MAIN until the simulation is to be terminated. The variable IHLF indicates whether the simulation has been terminated by HPCG due to numerical difficulties (IHLF = 11), in which case an error message is printed, or normally (IHLF = any other value).

The value of the acceleration due to gravity, kept in GRAV, sets the units of the simulation. Currently, GRAV = 386.4, which implies calculations in pounds, inches and seconds.

After initializing various constants, the operator is asked for the name of the output file, a run number which may be used to serialize the various simulations made, and a code which specifies whether and what intermediate output is to be printed. (See Reference 5 for output level code specifications.) MAIN then opens the output file and passes control to INPUT.

Upon return from INPUT, the vehicle parameters, initial positions and velocities, and sufficient bank profile points to span twice the vehicle wheelbase at the vehicles' initial position are in storage. MAIN then transfers the initial state variables into the array Y and fills DY with the error bounds used by HPCG in its step adjustment procedures. Currently, equal bounds in all degrees of freedom are used if a two axle vehicle is being simulated. Under current coding, the error bounds on the wheel positions and velocities for vehicles with more than two axles would be more stringent than the body degrees-of-freedom. This may not be the most advantageous weighing, but no further study of this has been made. The exact way of using these error bounds is given in the description of HPCG in the SSP manual.[13]

After initially filling Y and DY, MAIN sets the dimension of the equations of motion, writes the first output page title and headings and transfers control to HPCG.

Upon return from HPCG the simulation is terminated.

Subroutine INPUT

This subroutine reads the vehicle parameters, initial values and bank profile. INPUT first requests, from the operator, the vehicle data file name. INPUT then opens that file, reads it and echos each vehicle parameter onto the output file opened by MAIN. In the process, component masses are calculated from their weights.

After closing the vehicle file, the name of the bank profile file is requested from the operator. INPUT then opens that file, reads it, echos the bank title and soil parameters on the output file, and then reads XMIN (the x-coordinate of the first bank profile point given), DELTX (the distance, in inches, between successive bank profile points), and XMAX (the x'-coordinate of the last bank profile point given).

The span of the vehicle is next calculated by adding the radius of the first and last wheel to the wheelbase and stored in XLTRTB. This is the longest extent of the vehicle which can touch the bank. No vehicle body-bank interferences are considered; these should be added for future improvements.

Since the numerical integration, to be accurate and stable, "moves" the vehicle through small increments, only one vehicle span need be in core at any one time, as long as the bank profile directly under the vehicle is there. In order not to access to disk storage too frequently and yet not to use too much of core, two vehicle spans are initially read after the span has been calculated. XTMIN contains the x'-coordinate of the leftmost* bank profile point in core, XTMAX the x'-coordinate of the rightmost.

The array BNK contains the z'-coordinates (i.e., the elevations) of the bank; the first column, the original bank profile; the second column, the one after possible modification by vehicle travel. Initially, both

---

*For visualization, the vehicle is assumed to move from left to right with the bank extending from the lower left to the upper right.

columns are filled with the original bank profile by INPUT. After filling BNK with the initial two vehicle spans of the bank, INPUT requests the initial values from the operator. Here angles are converted from degrees (entered by the operator) to radians (used by the simulation).

Since the initial position of the vehicle need not be over the first two vehicle spans of the bank, the x-coordinate of the furthest possible forward part of the vehicle is checked against XTMAX, the rightmost bank profile point in core. If the bank in core does not extend over two vehicle spans at the initial vehicle position, more bank profile data is read (10 points at a time) until it does. If the end of the BNK storage array is reached before this happens, the entire bank profile is shifted leftward in BNK and more bank read.

After BNK contains the bank profile under the vehicle at its initial position, and XTMAX and XTMIN are adjusted appropriately, the number of bank profile points, KDTAU, and the radius of the largest wheel, DTAU, is calculated. Bank-wheel interference need only be checked for a distance DTAU on both sides of a wheel center x'-position.

INPUT then returns to MAIN.

Subroutine UPDATE

Subroutine UPDATE calculates the derivatives of the state variables whenever called upon to do so by HPCG. The inputs to UPDATE are the array Y and all the vehicle and bank parameters stored in COMMON. The output is the array DY containing:

$$DY(1) \quad = \quad \dot{u}$$

$$DY(2) \quad = \quad \dot{w}$$

$$DY(3) \quad = \quad \dot{Q}$$

$$DY(4) \quad = \quad \dot{q}_w$$

$$DY(5) \quad = \quad \dot{x}'_{CG} = u'$$

$$DY(6) \quad = \quad \dot{y}'_{CG} = w'$$

$$DY(7) \quad = \quad \dot{\theta} = Q$$

$$DY(7+i) \qquad = \dot{z}_i = z_{n_A+i}$$

$$DY(7+n_A+1) \quad = \ddot{z}_i$$

These are calculated from Equations 47 through 64. This is a rather long and complicated procedure encompassing all the calculations described in the section entitled EQUATIONS.

Since the subroutine is called at least twice per integration step, some concern must be made for execution time. A long and often unnecessary step in FORTRAN coding is the repeated use of subscripts. In UPDATE, whenever a subscripted variable must be used more than twice, it has been reassigned to a non-subscripted one. In fact, the first action of UPDATE is to transfer the state variables from the first seven locations of Y, which is subscripted, to the location called U, W, Q, QW, XCGP, ZCGP, and THETA. The parts of Y describing the axle motions are moved to subscripted variables called Z and ZD, where the calculations of each subscript involves two or three less operations than the subscripts of Y. Later, even the values in Z and ZD are moved to unsubscripted variables as necessary.

After the above reassignment, the wheel center positions in the bank coordinated system are calculated and stored in XP(I) and ZP(I). The corresponding velocities are stored in UP(I) and WP(I).

UPDATE then checks if the bank profile in core lies under the current position of the vehicle. At first it will, since INPUT adjusted it so, but after some time the vehicle will have moved rightward, requiring additional bank profile to be read in core. The procedure here is similar to that in INPUT. In case the vehicle should have moved left beyond the bank profile in core, an error message is printed and the simulation is terminated.

The next major task of UPDATE is the calculation of the entry and exit angles for each wheel with respect to the original bank profile and the current, or modified, bank profile. A test for wheel-bank contact is made by calculating the wheel surface position directly above each bank profile point for the distance DTAU on each side of the wheel center.

The test is made from left to right until a wheel surface point below the bank profile is found. If none is found until a distance DTAU on the right of the wheel center is found, no wheel-bank contact is made and all soil forces and wheel-soil variables are set to zero.

The first wheel surface point found below the bank elevation, testing from left to right, gives the wheel exit angle with respect to the particular bank. If the original bank profile is used, the angle so found is γ_{20} of Figures 5 and 6 which is stored in GAM2(I, 1). If the current bank profile is used, the angle found is γ_2 and is stored in GAM2(I, 2). The search for interference is then started from the right going to the left. The first wheel surface point below the bank elevation thus found yields the wheel entry angle γ_{10}, stored in GAM1(I, 1), or γ_1 stored in GAM1(I, 2). In all these cases, wheel-bank contact is assumed midway between the bank profile point below the wheel surface and the next one above the wheel surface. Coding is included, but not used, which allows more precise interpolation if required.

The location of the wheel-bank entrance and exit points are then calculated in the bank coordinates, and stored in X1G, Z1G and X2G, Z2G. From these, the local ground slope, stored in ST, is calculated and then the velocity of the wheel center parallel to this local ground slope is calculated and stored in UPG. Slip is then calculated by Equation 7.

The entrance and exit angles with respect to the current bank, the entrance angle with respect to the original bank, the ground angle, vehicle pitch angle and the state variables Y are now passed to the subroutine SOILF and the values of T_T of Equation 12, F_{sx} of Equation 17, F_{sz} of Equation 18 and M_{sx} of Equation 19 are returned for the wheel under consideration.

The buoyant forces and the drag on the rotating wheel are calculated next. In the program, A contains the area of the entire wheel under water, BB the part of the rim under water. Three cases are distinguished:

    1) the entire wheel or rim out of water,

    2) the entire wheel or rim under water, and

    3) part of wheel or rim under water.

The equations for Cases 1) and 2) are obvious. In Case 3) the area submerged is calculated using Equation 20. Wheel buoyancy is calculated using Equation 21 and stored in FBW(I).

To calculate rotational drag in Case 1) the drag is set to zero; in Case 2) Equation 22 is used directly; in Case 3) the proportion of the circumference under water is applied to Equation 22. The rotational drag of the Ith wheel is stored in QWDRG(I).

Engine RPM is now calculated from q_w for each gear starting at low gear and going to MAXGR, the highest gear to be used (requested by INPUT from the operator at initiation). Negative engine RPM results in an error message and the termination of the simulation. The lowest gear yielding an RPM below the upper shift point (in UPSRPM) is used as the operating gear. If no gear less than or equal to MAXGR yields an engine RPM below the maximum engine RPM, an error message is printed and the simulation is terminated. The engine RPM resulting from the operating gear is used to determine the engine torque by linear interpolation. Wheel torque is then calculated from Equation 24 and stored in WHLTRQ. Since it is assumed that there is no differential rotation among the wheels and all wheels are connected to the one engine on the vehicle, only one value of wheel torque is calculated and applied to all wheels.

The suspension forces are calculated next. The location of each wheel determines which of the Equations 25 is to be used and the spring force is calculated and stored in SPRGR. Similarly, a test is made to determine which of the Equations 26 is to be used for the damping force; it is calculated and then stored in DAMPF. The total suspension force is then calculated from Equation 27 and stored in D(I) for the Ith axle. The values used to describe the suspension forces are the sum of the forces acting on both sides of the axle.

The buoyant forces on the body are calculated by subroutine BBOX, described below. The buoyant force on box J is stored in FBB(J); the x-coordinate of the center of buoyancy of box J is stored in XCB(J); and the z-coordinate is stored in ZCB(J).

All the values required for the equations of motion have now been evaluated. Appearing in the equations of motion are 16 summations which are evaluated next. These are stored in the array SM according to the following scheme:[*]

$$SM(1) = \bar{M}_u = \sum M_{ui} z_i$$

$$SM(2) = \sum M_{ui} (I_y - \bar{M}_u z_i) \dot{z}_i$$

$$SM(3) = \sum M_{ui} (M z_i - \bar{M}_u) \dot{z}_i$$

$$SM(4) = \sum F_{bi}$$

$$SM(5) = \sum F_{sxi}$$

$$SM(6) = \sum M_{ui} (w - x_i Q)$$

$$SM(7) = \sum D_i$$

$$SM(8) = \sum D_i x_i$$

$$SM(9) = \sum M_{sxi}$$

$$SM(10) = \sum (T_{Ti} - D_{wi})$$

$$SM(11) = \sum F_{bi} z_i$$

$$SM(12) = \sum W_{ui} z_i$$

$$SM(13) = \sum M_{ui} (w - x_i Q) z_i$$

$$SM(14) = \sum F_{Bj}$$

$$SM(15) = \sum F_{Bj} z_{FBj}$$

$$SM(16) = \sum F_{Bj} x_{FBj}$$

---

[*]Note: In storage, $\dot{z}_i = z_{n_A + i}$, the summation over i goes from 1 to n_A; and the summation over j goes from 1 to n_B.

The above values, and others, are used to calculate F_x according to Equation 42, F_z according to Equation 44 and G_y according to Equation 46. Then the derivatives of the state variables are calculated according to Equations 60, 61, 62, 47, 49 and 50. The derivatives of the wheel position and velocity are calculated from Equations 63, 64 and 48.

Subroutine OUTPUT

Subroutine output, called by HPCG whenever an integration step is completed, determines if sufficient simulation time has passed to print an output or sufficient distance has been traveled to update the bank profile. If so, it takes the appropriate actions.

Since there is a variable number of lines in the output block (depending on the number of axles, n_A , and the number of body boxes, n_B) OUTPUT also checks if enough space is left on the current output page for another output block. If there is, it prints it; if not, it starts a new page and prints the run number, bank title and output block legend before the next output block.

Besides reporting on the progress of the simulation whenever necessary, OUTPUT also modifies the bank to conform to wheel travel. This cannot be done in UPDATE, since the equations of motion are often calculated for trial values of the integration interval. If, as a result of a trial value, the error made between the predictor and corrector (in HPCG) is too large or too small, the integration interval is modified and the equations of motion recalculated. If the bank had been modified in UPDATE, it would have to be restored when false integration steps are used. This would have been very complicated, and unnecessary.

HPCG continues to modify time increments until a successful integration step has been achieved. It then transfers control to OUTPUT. Now the bank profile can be modified to conform to the current wheel positions. This is done by determining all bank profile points at which bank-wheel interference occurs, and setting the bank elevation at the elevation of the wheel edge. This is done only with the current

bank profile stored in BNK(1, 2). The original bank, in BNK(1, 1) is left unmodified.

Subroutine SOILF

This subroutine, called for each axle, calculates the forces on the wheel and body due to wheel-soil interference. This coding is for the rigid wheel model described in Misklevitz.[6] The wheel is specified by the first variable in the calling sequence.

First, SOILF determines the appropriate soil parameters to be used for the current position of the wheel. It then calculates the maximum sinkage by Equation 4, and maximum normal stress by Equation 3. The coefficients (Equation 2) of the normal stress distribution given by Equation 1 are then calculated.

The integrals in Equations 8 and 9 are integrated analytically by Misklevitz.[6] The resulting formulas are used to calculate for the ith wheel $F_{x\sigma}$, stored in SIGH(I), and $F_{z\sigma}$, stored in SIGN(I).

Since the integrals of Equations 10 through 14 were not able to be evaluated analytically, a five point Newton-Coles formula[14] is used to evaluate them. The shear stresses at five angles between γ_1 and γ_2 was evaluated using Equations 5 and 6. Figure 20 shows the location of the five angles chosen for the numerical integration. These five angles were picked after considerations given by Misklevitz.[6] The five point Newton-Cotes formula then gave $F_{z\tau}$, stored in TAUN(I); $F_{x\tau}$, stored in TAUH(I); and T_τ, stored in TTAU(I).

F_{sx} (Equation 17) and F_{sz} (Equation 18) are then calculated.

Though somewhat more complicated, M_{sx} was calculated by a similar Newton-Cotes formula.

Subroutine BBOX

This subroutine calculates the buoyant forces and center of buoyancy of the vehicle body box specified by the first variable in the calling sequence.

After transferring the vehicle coordinates of the box corner to unindexed variables, their bank coordinates are calculated using Equation 29. A sequence of tests is then made to determine which of the cases described in section entitled <u>Body Buoyant Forces</u> applies.

The remainder of the coding of this subroutine follows the equations of that section so closely that no further explanation is needed.

FIGURE 20. TYPICAL SHEAR STRESS DISTRIBUTION
SHOWING POINTS USED IN NUMERICAL
APPROXIMATION OF ITS INTEGRAL
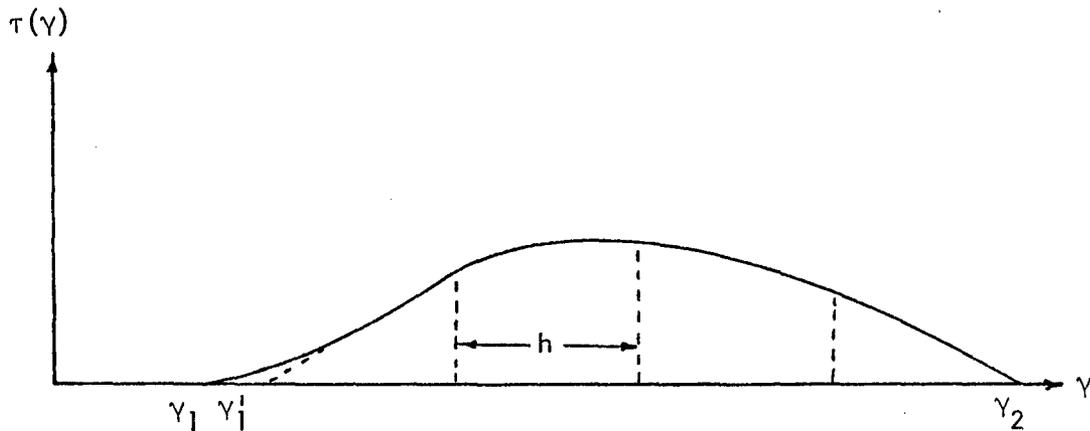
REFERENCES

1. Sloss, D., Ehrlich, I. R. and Worden, G., <u>Studies of Off-Road Vehicles in the Riverine Environment</u>, Vol. II, "An Analytical Method of Egress Evaluation," DL Report 1393, October 1969.

2. Ehrlich, I. R., Kamm, I. O. and Worden, G., <u>Studies of Off-Road Vehicles in the Riverine Environment</u>, Vol. I, "Performance Afloat," DL Report 1382, October 1968.

3. Ehrlich, I. R., Kolb, R. G., Sloss, D. A. and Corridon, L. M., <u>Studies of Off-Road Vehicles in the Riverine Environment</u>, Vol. III, "Associated Environmental Factors," DL Report 1285, April 1970.

4. Muddappa, S. K. and Baker, W. J., <u>Egress Performance of Amphibious Vehicles</u>, U. of Detroit, August 1971.

5. Jurkat, M. P., <u>User's Manual for EGRES3.F4 and BNKPRO.F4</u>, DL Report Report SIT-DL-73-1685, July 1973.

6. Miszklevitz, S. L., "A Dynamic Simulation of Soil-Wheel Interaction," DL Report SIT-DL-73-1689, September 1973.

7. Bekker, M. G. <u>Introduction to Terrain-Vehicle Systems</u>, Ann Arbor, U. of Michigan Press, 1969.

8. Janosi, Z. and Hanamoto, B., "The Analytical Determination of Drawbar Pull as a Function of Slip for Tracked Vehicles in Deformable Soils," <u>Proceedings of the First International Conference on the Mechanics of Soil Vehicle Systems</u>, Paper No. 44, Editzione Muerva Technica, Turin, Italy, 1962.

9. Schuring, D. and M. R. Belsdorf, <u>Analysis and Simulation of Dynamical Vehicle-Terrain Interaction</u>, T. M. CAL No. VJ-2330-G-56, Cornell Aeronautical Laboratory, May 1969.

10. Ehrlich, I. R. and Nuttall, C. J., <u>Preliminary Studies of a Wheel Pump for the Propulsion of Floating Vehicles</u>, DL Report SIT-DL-69-1419, December 1969.

11. Etkin, B., <u>Dynamics of Flight</u>, New York, John Wiley and Sons, Inc., 1959.

12. Jurkat, M. P., <u>Background Notes in Vehicle Dynamics</u>, DL Report SIT-DL-70-1466, June 1970.

13. IBM Manual: System/360 Scientific Subroutine Package (36Ø A-CM-Ø3X)
     Version III, Programmer's Manual H2Ø-Ø2Ø5-3.

14. Hamming, R. W., Numerical Methods for Scientists and Engineers, 2nd
     Edition, New York, McGraw-Hill, Inc., 1973.

NOMENCLATURE

Unprimed variables measured in vehicle coordinate.

Primed variables measured in earth-fixed coordinate.

Dots above variables mean differentiation with respect to time.

Subscripts

b	wheel buoyancy
B	refers to body buoyancy
c	wheel compression (or jounce) direction
CG	center of gravity of sprung mass
G	parallel to local ground slope or refers to transmission
i	wheel index, $i = 1, \ldots n_A$; gear index $i = 1, \ldots, N_G$
d	damper
p	spring
r	wheel rebound direction
R	rim, wheel rest position, engine speed, rectangle
T	triangle
s	soil, submerged, or sprung mass
u	upper suspension bump stop, or unsprung mass
x	in vehicle x-direction
z	in vehicle z-direction
γ	at point on wheel surface located by a line from wheel center making an angle γ with respect to horizontal
j	body box index, $j = 1, \ldots, n_B$; or box corner index, $j = 1,2,3,4$
ℓ	lower suspension bump stop
ω	wheel
σ	arising from soil-wheel normal force
τ	arising from soil-wheel shear force

Nomenclature
(cont'd)

Variables

a,b	parameters of wheel rotational drag equations
$A_{abc...}$	area designated by subscripts a,b,c,...
A,B,C	points used in vehicle body buoyancy locations or coefficients of normal stress equations
b	wheel width
c,φ	Coulomb soil shear strength parameter
d_r, d_c	wheel damper (shock absorber) constant
D	total suspension force
D_w	wheel rotational drag
E_{Ri}	engine speed in i^{th} gear
$F_{abc...}$	force designated by subscripts a,b,c,...
F_{dr}, F_{dc}	maximum force derivable from wheel dampers (blow-off force)
G_F	final drive ratio
G_i	gear ratio of ith gear
G_y	total applied moment about CG
h	height of box
I_y, I_{ys}	pitch moment of inertia of total vehicle and sprung mass
j	soil deformation
k	spring constant or soil deformation parameter
k_c, k_φ, n	Bekker's soil strength parameters
k_u, k_ℓ	spring constant of upper and lower bump stops
M	total vehicle mass
$M_{abc...}$	moments or masses designated by subscripts a,b,c,...
$\bar{M}_u$	total mass moment of unsprung masses
n_B	number of body boxes
n_A	number of axles
n_G	number of transmission gears

Nomenclature
(cont'd)

Variables

P_i	bank profile location points (in x'-z' coordinates)
Q	vehicle pitch velocity (positive nose rising)
q_w	wheel rotational velocity (positive when wheel bottom moving towards rear of vehicle)
r	wheel radius
s	wheel rotational slip
S_i	bank x'-coordinates at which one or more soil parameters change
S_p, S_d	spring force due to spring and damper
S_R	engine speed at which next lower gear is selected
s_w	slope of waterline with respect to vehicle coordinate
$T_{abc\ldots}$	torques designated by subscripts a,b,c,$\ldots$
T_E	engine torque
T_ω	torque at wheels
u	vehicle surge velocity (positive forward)
u_G	velocity of wheel center parallel to local ground slope
U_R	engine speed at which next higher gear is selected
w	vehicle heave velocity (positive down)
w_B	width of body buoyancy boxes
x	surge direction moving with vehicle (positive forward)
x'	bank coordinate parallel to water surface (positive bankward from water bank intersection)
x_{FB}	x-coordinate of box center of buoyancy
z	heave direction moving with vehicle (positive down)
z'	bank coordinate perpendicular to water surface (positive down for water surface)
z_{FB}	z-coordinate of box center of buoyancy
z_i, z_i'	location of center of wheel i

Nomenclature
(cont'd)

Variables

z_ℓ wheel center position when lower bump stop is first contacted

z_m wheel sinkage of center of contact patch

z_R wheel center position when spring is extended to its no-force distance

z_u wheel center position when upper bump stop is first contacted

z_w z-intercept of waterline in vehicle coordinates

α angle defined by $\pi/2 + \gamma - \theta$

η_G, η_F efficiencies of transmission and final drive

γ angle made by line connecting wheel center with a point in the contact patch

γ_1 entry angle of wheel with respect to modified bank

γ_2 exit angle of wheel with respect to modified bank

γ_{10} entry angle of wheel with respect to original bank

γ_{20} exit angle of wheel with respect to original bank

ℓ length of box

ρ density of water

σ soil-wheel normal stress

τ soil-wheel shear stress

θ pitch rotational translation moving with vehicle (positive nose up measured from x-axis)

θ_G local bank slope

θ_ω angle with respect to vertical made by line from wheel center to wheel-water intersection

DISTRIBUTION LIST

36   Commander
U. S. Army Tank-Automotive Command
Warren, Michigan 48090

ATTENTION:

Chief Scientist, AMSTA-CL   (1)
Director of RD&E, AMSTA-R   (1)
Deputy Director of RD&E, AMSTA-R   (1)
Foreign Intelligence Office, AMSTA-RI   (1)
Systems Development Division, AMSTA-RE   (1)
Concept & Technology Division, AMSTA-RH   (1)
Vehicular Components Division, AMSTA-RK   (1)
Surface Mobility Division, AMSTA-RU   (1)
Research & Analysis Functions, AMSTA-RUR   (20)
Propulsion Systems Division, AMSTA-RG   (1)
Canadian Forces Liaison Office, CDLS-D   (1)
U. S. Marine Corps Liaison Office, USMC-LNO   (1)
Project Manager ARSV, AMCPM-RSV   (1)
Project Manager MICV, AMCPM-MICV   (1)
Project Manager M561, AMCPM-GG   (1)
Project Manager M60, AMCPM-M60   (1)
Project Manager XM1, AMCPM-GCM   (1)

4   Office, Chief of Research & Development
Department of the Army
ATTN: LTC F. Trevino, Mr. M. V. Kreipke,
       Dr. V. Zadnik, LTC W. Prime
Washington, D. C. 20310

2   Commander
U. S. Army Weapons Command
ATTN: AMSWE-SY (Dr. Hung, Mr. Rankine)
Rock Island, Illinois 61201

2   Director
U. S. Army Corps of Engineers
Waterways Experiment Station
P. O. Box 631
Vicksburg, Mississippi 39180

Distribution List

No. of
Copies

6   Director
U. S. Army Corps of Engineers
Waterways Experiment Station
ATTN: Mobility & Environmental Laboratory
P. O. Box 631
Vicksburg, Mississippi 39180

1   Superintendant
U. S. Military Academy
ATTN: Professor of Ordnance
West Point, New York 10996

1   Director
U. S. Army Natick Laboratories
ATTN: Technical Library
Natick, Massachusetts 01760

2   Commander
U. S. Army Materiel Command
AMC Building, Room 8S56
ATTN: Mr. R. Navarin, AMCRD-TV
Washington, D. C. 20315

1   Commander
U. S. Army Materiel Command
ATTN: AMCRD-GV, Mr. J. Carr
Washington, D. C. 20315

1   President
U. S. Army Arctic Test Center
ATTN: STEAC-IT (Mr. Dufendach)
APO 409
Seattle, Washington 98733

2   Commander
U. S. Army Test & Evaluation Command
ATTN: AMSTE-BB and AMSTE-TA
Aberdeen Proving Ground, Maryland 21005

2   Director
U. S. Army Ballistic Research Laboratory
Aberdeen R&D Center
Aberdeen Proving Ground, Maryland 21005

Distribution List

No. of
Copies

3 Director
U. S. Army Cold Regions Research & Engineering Lab
ATTN: Dr. W. Harrison, Dr. D. Freitag, Dr. R. Liston
P. O. Box 282
Hanover, New Hampshire 03755

1 Commander
U. S. Army Combat Development Command
ATTN: Mr. E. Hurford
Fort Lee, Virginia 23801

1 Director
U. S. Army Human Engineering Laboratory
ATTN: Mr. Eckels
Aberdeen Proving Ground, Maryland 21005

2 Grumman Aerospace Corporation
ATTN: Dr. L. Karafiath, Mr. E. Markow
Plant 35
Bethpage, Long Island, New York 11714

1 Dr. Bruce Liljedahl
Agricultural Engineering Department
Purdue University
Lafayette, Indiana 46207

1 Mr. T. Andrisan
Brown Engineering Corporation
Huntsville, Alabama 35804

2 Director
U. S. Army Advanced Materiel Concepts Agency
ATTN: Mr. Rymiszewski, Mr. Kurtz
5001 Eisenhower Avenue
Alexandria, Virginia 22304

1 Dr. W. G. Baker
Civil Engineering Department
University of Detroit
4001 W. McNichols
Detroit, Michigan 48221

Distribution List

No. of
Copies

1   Director
        U. S. Army Transportation Agency
        ATTN: CDCT-M (Mr. Betts)
        Fort Eustis, Virginia 23604

1   Professor E. Niemi
        Keweenaw Field Station
        Rural Route 1
        P. O. Box 94D
        Calumet, Michigan 49913

3   Director
        U. S. Army Materiel Systems Analysis Agency
        ATTN: Messrs. D. Woomert, W. Niemeyer, W. Criswell
        Aberdeen Proving Ground, Maryland 21005

2   Library
        Cornell Aeronautical Laboratory
        Box 235
        4455 Genessee Street
        Buffalo, New York 14221

2   Director
        National Tillage Machinery Laboratory
        Box 792
        Auburn, Alabama 36830

2   Chrysler Corporation
        Mobility Research Laboratory, Defense Engineering
        ATTN: Dr. B. Van Deusen, Mr. J. Cohren
        Dept. 6100
        P. O. Box 751
        Detroit, Michigan 48231

1   Dr. N. C. Costes
        George C. Marshall Space Flight Center
        Code SSE-SSL-N
        Huntsville, Alabama 35809

12   Director
        Defense Documentation Center
        Cameron Station
        Alexandria, Virginia 22314

Distribution List

No. of
Copies

2	President U. S. Armor Board Fort Knox, Kentucky 40121
1	Food Machinery Corporation 1105 Coleman Avenue P. O. Box 267 Technical Library San Jose, California 95103
1	Commander HQ, U. S. Air Force (SAGT) ATTN: Major Goodel Washington, D. C. 20330
1	Southwest Research Institute ATTN: Mr. R. C. Hemion 8500 Culebra Road San Antonio, Texas 78228
1	U. S. Marine Corps Mobility & Support Division Development and Education Command ATTN: Mr. S. Hickson Quantico, Virginia 22134
1	Mr. H. C. Hodges Nevada Automotive Test Center Box 234 Carson City, Nevada 89701
1	Mr. W. S. Hodges Lockheed Missile and Space Corporation R&D Division Sunnyvale, California 94088
2	Commander Yuma Proving Ground ATTN: STEYP-RPT, STEYP-TE Yuma, Arizona 85364
1	Mr. A. M. Wooley West Coast Test Branch Mobility and Support Division Marine Corps Base Camp Pendleton, California 92055

Distribution List

No. of
Copies

1 Mr. R. D. Wismer
Deere & Company
Engineering Research
3300 River Drive
Moline, Illinois 61265

1 U. S. Forest Service
Division of Engineering
ATTN: Mr. B. Y. Richardson
1621 N. Kent Street
Arlington, Virginia 22209

1 Mr. Irja Johnsson
SFM, Forsvaretsforskningsanstalt
Avd 2
Stockholm 80, Sweden

1 Oregon State University
Library
Corvallis, Oregon 97331

1 Mr. Sven E. Lind
SFM, Forsvaretsforskningsanstalt
Avd 2
Stockholm 80, Sweden

1 Mr. Robert W. Forsyth
Lockheed Aircraft Service Company
P. O. Box 33
Ontario, California 91764

1 Engineering Societies Library
345 East 47th Street
New York, New York 10017

1 Dr. M. G. Bekker
224 East Islay Drive
Santa Barbara, California 93101

2 Dr. I. R. Ehrlich
Stevens Institute of Technology
Davidson Laboratory
Castle Point Station
Hoboken, New Jersey 07030

2 Mr. C. J. Nuttall, Jr.
Chief, Mobility Research Branch
U. S. Army Engineers Waterways Experiment Station
Vicksburg, Mississippi 39181

REPORT DOCUMENTATION PAGE	READ INSTRUCTIONS BEFORE COMPLETING FORM	
1. REPORT NUMBER SIT-DL-74-1686	2. GOVT ACCESSION NO.	3. RECIPIENT'S CATALOG NUMBER
4. TITLE *(and Subtitle)* MATHEMATICAL MODEL OF WHEELED VEHICLES EXITING FROM THE RIVERINE ENVIRONMENT	5. TYPE OF REPORT & PERIOD COVERED FINAL	
	6. PERFORMING ORG. REPORT NUMBER	
7. AUTHOR(s) M. Peter Jurkat	8. CONTRACT OR GRANT NUMBER(s) DAAE07-73-C-0056	
9. PERFORMING ORGANIZATION NAME AND ADDRESS Davidson Laboratory 711 Hudson Street Hoboken, N. J. 07030	10. PROGRAM ELEMENT, PROJECT, TASK AREA & WORK UNIT NUMBERS	
11. CONTROLLING OFFICE NAME AND ADDRESS U. S. Army Tank-Automotive Command Warren, Michigan 48090	12. REPORT DATE February 1974	
	13. NUMBER OF PAGES 60	
14. MONITORING AGENCY NAME & ADDRESS*(if different from Controlling Office)*	15. SECURITY CLASS. *(of this report)* UNCLASSIFIED	
	15a. DECLASSIFICATION/DOWNGRADING SCHEDULE	

16. DISTRIBUTION STATEMENT *(of this Report)*

Approved for public release; distribution unlimited.

17. DISTRIBUTION STATEMENT *(of the abstract entered in Block 20, if different from Report)*

18. SUPPLEMENTARY NOTES

19. KEY WORDS *(Continue on reverse side if necessary and identify by block number)*

River Crossings   Amphibians   Computer Simulation

Mobility   Off-Road Vehicles

20. ABSTRACT *(Continue on reverse side if necessary and identify by block number)*

DAVIDSON LABORATORY, Stevens Institute of Technology
Hoboken, N. J. 07030

MATHEMATICAL MODEL OF WHEELED VEHICLES EXITING
FROM THE RIVERINE ENVIRONMENT

Final Report SIT-DL-74-1686. 60 pp., 20 figures.

M. Peter Jurkat. February 1974.

Contract DAAE07-73-C-0056. Prepared for the
U. S. Army Tank-Automotive Command. DL Project 4026/453.

[Approved for public release; distribution unlimited]